Univerzita Karlova v Praze

Přírodovědecká fakulta

Studijní program: Biologie

Studijní obor: Buněčná a vývojová biologie

Bc. Vojtěch Dostál

Analysis of WASH complex component FAM21

Analýza FAM21, podjednotky WASH komplexu

Diplomová práce

Školitel: RNDr. Lenka Libusová, Ph.D.

Praha, 2015

Prohlášení

Prohlašuji, že jsem závěrečnou práci zpracoval samostatně a že jsem uvedl všechny použité informační zdroje a literaturu. Tato práce ani její podstatná část nebyla předložena k získání jiného nebo stejného akademického titulu.

V Praze, 1. 5. 2015

_____

Vojtěch Dostál

Contents

Abstract 1
1. Theoretical background 2
1. 1. Actin cytoskeleton 2
1. 2. Actin assembly factors 3
1. 3. Arp2/3 nucleation-promoting factors 3
1. 3. 1. WASP 5
1. 3. 2. WAVE 5
1. 3. 3. Other nucleation-promoting factors 5
1. 4. WASH complex 6
1. 4. 1. WASH 7
1. 4. 2. Strumpellin 7
1. 4. 3. SWIP 8
1. 4. 4. CCDC53 8
1. 5. FAM21 8
1. 5. 1. FAM21 localization 10
1. 5. 2. FAM21 on endosomes 10
1. 5. 3. FAM21 at the plasma membrane 13
1. 5. 4. FAM21 in the nucleus 13
1. 6. Interaction partners of FAM21 13
1. 6. 1. WASH complex components 14
1. 6. 2. Retromer 15
1. 6. 3. CCDC22 and CCDC93 16
1. 6. 4. FKBP15 17
1. 6. 5. RME-8 17
1. 6. 6. SNX27 17
2. Goals 18
3. Experimental procedures 18
3. 1. Materials 18
3. 1. 1. Media and buffer solutions 18
3. 1. 2. Antibodies 23
3. 1. 3. Constructs 24
3. 2. Human cell line experiments 24
3. 2. 1. Cell culture 24

3. 2. 2. Transfection and pre-treatments 24
3. 2. 3. SDS PAGE/Western blot 25
3. 2. 4. Immunofluorescence 26
3. 2. 5. Microscopy 26
3. 2. 6. Quantitative PCR 28
3. 3. *Dictyostelium* experiments 29
3. 3. 1. Cloning 29
3. 3. 2. *Dictyostelium* cell culture 30
3. 3. 3. *Dictyostelium* transfection 30
3. 3. 4. Crosslinking assay 30
3. 3. 5. GST pulldown 32
4. Results 33
4. 1. Overexpression and endogenous protein detection of FAM21 in U2OS cell line 33
4. 2. Localization of FAM21 to the early endosomes 35
4. 3. FAM21 in non-early endosomal compartments 38
4. 4. New interaction partners of FAM21 in *D. discoideum* 41
4. 5. Binding partners of the LFa motifs of FAM21 45
4. 6. Experiments on Vps35 – FAM21 association in U2OS 48
5. Discussion 49
5. 1. FAM21 localization 50
5. 2. FAM21 interaction partners 52
5. 3. Endosomal attachment of FAM21 56
6. Conclusion 58
7. Acknowledgements 59
8. Abbreviations 59
9. References 62
9. Supplementary information ..... **Chyba! Záložka není definována.**

Abstract

The dynamics and function of the actin cytoskeleton depends on polymerization and branching of actin filaments, an event that is stimulated by Arp2/3. Arp2/3-dependent branching is closely linked to the pentameric WASH complex which consists of WASH, strumpellin, SWIP, CCDC53 and FAM21. WASH complex is associated mainly with endosomes. It was traditionally localized to retromer-coated domains of early endosomes which enable sorting and recycling of endocytosed material. However, latest scientific data extend the role of WASH complex to other endosomal or even non-endosomal sites. Of all the subunits of the WASH complex, FAM21 is the most prominent hub for protein-protein interactions, thanks to its long unstructured C-terminal domain. In my diploma thesis FAM21 was localized to early and late endosomes and lysosomes of U2OS human cell line. *Dictyostelium discoideum* was then used as a model organism to investigate FAM21 protein interactions as well as the proteins associated specifically with the C-terminal domain of FAM21. Results of the study shed new light on the complex network of FAM21 interactions and question the long-standing theories on the function of WASH complex in cells.

Abstrakt

Dynamika a větvení aktinové sítě je stimulována komplexem Arp2/3. Ten může být regulován WASH komplexem, který se skládá z proteinů WASH, strumpellin, SWIP, CCDC53 a FAM21. WASH komplex je v buňce asociován především s endozómy. Dříve se předpokládalo, že WASH komplex lokalizuje téměř výhradně na retromerické domény časných endozómů, které umožňují třídění a recyklaci endocytovaného materiálu. Nejnovější poznatky rozšiřují pole působnosti WASH komplexu i do jiných typů endozómů či dokonce do zcela odlišných buněčných kompartmentů. Z pěti podjednotek WASH komplexu je FAM21 zřejmě nejvýznamnějším vazebným partnerem pro další proteiny, které s WASH komplexem interagují – a to díky neobvykle dlouhé nestrukturované C-terminální doméně. FAM21 do časných, ale i pozdních endozómů a lysozómů buněčné linie U2OS. Následně byly pomocí modelu *Dictyostelium discoideum* hledáni noví interakční partneři FAM21 i proteiny asociované s částí C-terminální domény FAM21. Studie přináší nové poznatky týkající se interakční sítě proteinu FAM21 a zpochybňuje některé dlouho uznávané modely funkce WASH komplexu v buňkách.

1. **Theoretical background**

The actin cytoskeleton is a complex and dynamic system assembling around the actin microfilaments. There is hardly any aspect of cellular physiology where the actin cytoskeleton does not play a role – including cell migration, division, but also cell signalling and vesicular transport. The actin network depends on regulatory proteins which allow it to form complex branched structures needed to fulfil the diverse physiological roles in cell. WASH complex is one of these master regulators.

1. 1. Actin cytoskeleton

Actin was first purified from muscle tissue as a counterpart of myosin that is required for its contractile action - hence the name, actin (Straub, 1942). This was followed by findings that monomeric actin (G-actin) polymerizes into a filamentous form (F-actin) and binds adenosine triphosphate (ATP) which is actually important for the assembly of actin into polymers (Astbury et al., 1947; Straub and Feuer, 1950). With 375 amino acids, actin is so conserved that the human and chicken homologues have identical protein sequence (Reisler and Egelman, 2007). A three-dimensional model of G-actin has provided insight into the structure of this peculiar protein, which consists of two major domains and a nucleotide-binding cleft in between (Kabsch et al., 1990).

G-actin readily assembles into the helically filamentous F-actin but the assembly is reversible and so the equilibrium between G- and F-actin is dynamic. Often, actin filaments grow at one end while disassembling at the other, leading to a process called treadmilling (Wegner, 1976). Importantly, ATP is a timer which regulates this dynamics: when in F-actin, ATPase activity of actin is increased >40,000-fold and the resulting ADP + Pi (adenosine diphosphate and inorganic phosphate) are released from actin. Such molecular event in turn promotes F-actin disassembly (Blanchoin and Pollard, 2002).

Given the various roles attributed to actin in cells, it is not surprising that it is under a control of a multitude of actin-binding and associated proteins. The last systematic review on this topic counted 162 distinct proteins which bind actin in mammalian cells. Some of these bind G-actin and sequester it, others bind to F-actin along the length of the filament or associate with filament ends (dos Remedios et al., 2003). For instance, complex actin structures such as lamellipodia and microvilli require a substantial amount of crosslinking and branching of individual

microfilaments. Such branching events are promoted by a group of actin associated proteins which are collective called the “actin assembly factors” (Chhabra and Higgs, 2007).

1. 2. Actin assembly factors

Actin microfilaments can grow by addition of individual G-actin subunits to the “barbed” (fast-growing) end. However, *de novo* assembly (nucleation) of an actin oligomer is a rare biochemical event which represents a rate-limiting step of actin polymerization (Firat-Karalar and Welch, 2011). In agreement with experimental studies, computer simulations showed that formation of actin dimers is unfavourable and a barrier must be overcome to form an actin trimer, the critical nucleus size (Sept and McCammon, 2001).

At the time these computer simulations were undertaken, a very probable explanation had already been published. A complex of actin-related proteins 2 and 3 (Arp2/3) was found to bind to the sides of actin polymers and nucleate the growth of new actin oligomers by forming F-actin branches at an angle of 70° from the pre-existing filaments (Mullins et al., 1998). Arp2 and Arp3, together with five other auxiliary polypeptides, thus form a stable nucleation core from which actin can polymerize, removing the need for actin dimers in the process of actin nucleation (Kelleher et al., 1995; Machesky et al., 1994).

Several other actin assembly factors besides Arp2/3 have been described to date. Formins are a class of proteins able to associate with the growing ends of actin filaments and promoting assembly of very long microfilaments which would otherwise never reach such lengths (Kovar, 2006). Spire is a newly discovered assembly factor with a potency to nucleate actin filaments by conjoining four actin monomers in a row (Baum and Kunda, 2005). There is a state-of-the-art equilibrium between the Arp2/3- and formin-assembled microfilament populations. Disruption of Arp2/3 functionality promotes formin-based nucleation, and vice versa (Burke et al., 2014).

Arp2/3 complex alone has low nucleation activity towards actin. Besides ATP, which is clearly required for Arp2/3 activity (Dayel et al., 2001), additional cellular factors have been discovered (Rohatgi et al., 1999). These are often called nucleation-promoting factors because they increase the activity of Arp2/3, and will be the focus of the next few paragraphs.

1. 3. Arp2/3 nucleation-promoting factors

Arp2/3 activation regulates formation of cell protrusions or adherens junctions, endocytosis, endosomal fission and cytoplasmic streaming, all by triggering actin assembly (Rotty et al.,

2013). It is clear that Arp2/3 activation must be kept on a tight leash to prevent unwanted actin polymerization.

Activation of Arp2/3 is mostly mediated by nucleation-promoting factors (NPFs) of the Wiscott-Aldrich syndrome protein (WASP) family (**Figure 1**). These range from the canonical WASP and WAVE/SCAR (WASP family Verprolin-homologous protein/Suppressor of cAMP receptor) to enigmatic WASH (Wiscott-Aldrich Syndrome Homology), JMY (Junction-mediating and regulatory protein) and WHAMM (WASP homolog-associated protein with actin, membranes and microtubules). Many of the proteins are well conserved among eukaryotic species (for review see Rottner et al., 2010; Veltman and Insall, 2010), underlining their importance.

Figure 1 – WASP family NPFs in cell physiology. Nucleation promoting factors regulate diverse aspects of cell movement and migration as well as vesicular transport. Adapted from Campellone and Welch, 2010.

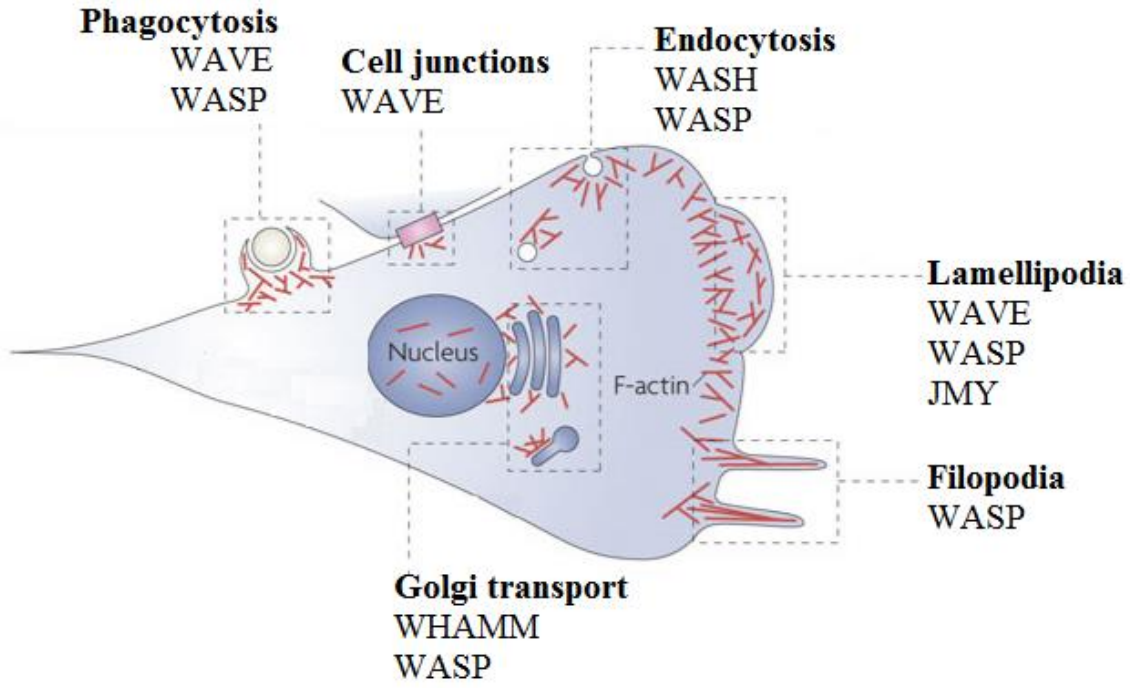

Activity of NPFs is overseen by a multitude of cellular factors. Small Rho-family GTPases such as Rac1 and Cdc42 are known to play an important role, at least in some cases. Activated GTPases bind to NPFs and promote binding of Arp2/3. The specificity of various GTPases

towards NPFs has not been resolved yet (Tomasevic et al., 2007) and some NPFs were not assigned a GTPase at all.

1. 3. 1. WASP

WASP is a founding member of the WASP family and gene encoding the WASP protein was first isolated in 1994 from patients suffering from Wiscott-Aldrich syndrome, a genetic disease associated with thrombocytopenia, eczema and immunodeficiency (Derry et al., 1994). Several functional domains are present in the protein sequence of WASP, including a GTPase-binding region (which recruits Rho-like GTPases), a proline-rich region (that associates with several proteins including profilin which in turn promotes actin polymerization) and a verprolin/cofilin-homology domain (also known as verprolin-connector-acidic [VCA] module) which binds to actin and Arp2/3 (Goley and Welch, 2006; Nonoyama and Ochs, 1998).

WASP serves as an interface between signalling receptors and actin cytoskeleton (Nonoyama and Ochs, 1998). It has a role in the formation of filopodia, thin cell protrusions (Pollitt and Insall, 2009) and is indispensable for the biogenesis of invadopodia, membrane structures extending into the extracellular matrix and mediating its degradation (Lorenz et al., 2004; Gligorijevic et al., 2012). Some studies also suggest a role in clathrin-mediated endocytosis (Galovic et al., 2011).

1. 3. 2. WAVE

WAVE, also called SCAR because it was independently named by two groups, is another protein with an actin- and Arp2/3-binding VCA module (Bear et al., 1998; Miki et al., 1998). In cells, it co-immunoprecipitates with four proteins (Sra1, Nap1, Abi, HSPC300) and these, together with WAVE, constitute a heteropentameric WAVE complex (Eden et al., 2002; Jia et al., 2010). The WAVE complex is intrinsically inactive but inducible by Rac GTPase (Ismail et al., 2009). WAVE is required for the formation of lamellipodia, broad protrusions of the cell membrane (Kunda et al., 2003).

1. 3. 3. Other nucleation-promoting factors

The biological significance of other NPFs is known to a lesser extent. WASH localizes to endosomes and regulates their shape and scission, while WHAMM knock-down causes defects in endoplasmic reticulum (ER)-to-Golgi transport (for review see Rottner et al., 2010; Rotty et al., 2013). JMY is a dual-function protein which activates Arp2/3 and promotes cell migration but also has an unrelated p53-dependent role in the nucleus (Zuchero et al., 2009). So far,

"class I" NPFs were only mentioned but "class II" NPFs are also increasingly recognized (Goley and Welch, 2006). Among them, cortactin is a potent Arp2/3 stimulator which acts synergistically with WASP at the leading edge of migrating cells and at invadopodia (Oser et al., 2009; Weaver et al., 2001). Other class II NPFs include yeast proteins Abp1 and Pan1 (Goley and Welch, 2006).

1. 4. WASH complex

WASH was described rather recently in the subtelomeric region of the human genome (Linardopoulou et al., 2007). In 2009, two groups published a finding that WASH is present in cells in a multi-subunit complex (hence referred to as the WASH complex[1]) and siRNA silencing of WASH leads to exaggerated tubularization of the endosomal network (Derivery et al., 2009; Gomez and Billadeau, 2009). The knock-down phenotype was not observed in knock-out cell lines of WASH (Gomez et al., 2012) but the endosomal role of the WASH complex has been established. WASH complex members were confirmed and named as FAM21 (formerly KIAA0592), strumpellin (formerly KIAA0196), SWIP (formerly KIAA1033) and CCDC53 (Jia et al., 2010), establishing a pentameric model of WASH complex structure. The WASH complex is structurally related to the WAVE complex and four of their five subunits show certain amount or similarity. Interestingly, the only component of WASH complex which has no apparent counterpart in WAVE is FAM21 (Jia et al., 2010), a large and structurally unusual protein which is the principal topic of this thesis.

WASH complex is required for at least two vesicular trafficking pathways – the endosome-to-Golgi pathway and the endosome-to-cell surface retrieval (Seaman et al., 2013). The defining feature of the WASH complex is its prominent localization to early endosomes. It plays a major role in the sorting and quick recycling compartment of early endosomes (Derivery et al., 2009). This is unlike the other WASP family proteins which mainly localize to the leading edge of migrating cells (Nozumi et al., 2003; Sukumvanich et al., 2004). WASH complex stimulates endosome-to-Golgi recycling of cation-independent mannose phosphate receptor [CI-MPR] (Gomez and Billadeau, 2009; McGough et al., 2014a), α5β1 integrin recycling from endosomes (Zech et al., 2011), V-ATPase recycling from late endosomes to recycling vesicles (Carnell et al., 2011), transport of autophagy-related protein 9A (ATG9A) from the Golgi

[1] From now on, "WASH complex" is always referred to as WASH complex; "WASH" refers to one of the protein subunits of the WASH complex.

apparatus to the autophagosome (Zavodszky et al., 2014), endosome-to-plasma membrane recycling of major histocompatibility complex II [MHCII] (Graham et al., 2014) and, according to some authors, also endosome-to-plasma membrane retrieval of transferrin receptor (Zech et al., 2011) and glucose transporter 1 [GLUT1] (Zavodszky et al., 2014). The spectrum of influenced pathways is thus very wide. WASH complex usually works together with the retromer complex which will be discussed later. However, at least some publications suggest that not all retromer-dependent cargo also requires the WASH complex (McGough et al., 2014b). An emerging concept is that WASH, together with other components of the WASH complex, plays an intricate and multifaceted role in the regulation of the cellular physiology, at endosomes but also in other places (Deng et al., 2014; King et al., 2013).

The next five subchapters will briefly describe each component of the WASH complex independently of the others.

1. 4. 1. WASH

Human genome contains at least seven copies of WASH but only one of them (WASH1, 465 amino acids) is not truncated by frameshifts or premature in-frame stop codons. The most conserved portion of the protein, located at the C-terminus, contains a polyproline stretch followed by a "VCA module" similar to that seen in other WASP family proteins. The N-terminal portion of the protein is less conserved among eukaryotes but includes two recognizable domains, the WASH homology domain 1 and 2, abbreviated as WHD1 and WHD2, respectively (Linardopoulou et al., 2007). Recombinant WASH is intrinsically active (and stimulates Arp2/3 to promote actin assembly) but is largely present in an inhibited, inactive conformation when associated with the rest of the WASH complex (Jia et al., 2010). Efforts to identify WASH activators (such as a GTPase) have been largely fruitless although Rho1 was recently shown to bind and regulate WASH in a subset of *Drosophila* immune cells (Verboon et al., 2015). Another recent finding is WASH activation by a Tripartite motif 27 (TRIM27) ubiquitin ligase. This RING-family enzyme (where RING stands for "Really Interesting New Gene") catalyzes the ubiquitination of lysine 220 of human WASH. The process, which is thought to activate WASH, is stimulated by protein MAGE-L7, which belongs to an elusive melanoma antigen (MAGE) family (Hao et al., 2013).

1. 4. 2. Strumpellin

Strumpellin is a protein with 1,159 amino acids whose mutations were causatively linked to hereditary spastic paraplegia. Degeneration of corticospinal tract neurons (with axons

exceeding 1 meter in length) is a hallmark of the disease (Valdmanis et al., 2007). Not much is known about strumpellin besides the fact that it is a component of the WASH complex. The protein has no identifiable domains except for a spectrin fold that is thought to enable transient interactions with cytoskeleton. Disease-causing mutations could provide a clue to strumpellin function. However, expression of the mutant strumpellin does not destabilize the WASH complex or alter its localization; it is speculated that the mutations might instead obstruct binding of unknown additional interacting proteins (Freeman et al., 2013). Interestingly for future research, phosphatidylinositol-4-kinase type IIα and BLOC-1 complex constituents have recently been shown to co-immunoprecipitate strongly with strumpellin (Ryder et al., 2013).

1. 4. 3. SWIP

Like strumpellin, SWIP (strumpellin and WASH-interacting protein) is 1,173 amino acids long and has no recognizable domains. It is also genetically linked to a serious human disease – a subtype of autosomal recessive intellectual disability (Ropers et al., 2011). Interestingly, SWIP is the only WASH complex components whose knock-out can delocalize other WASH complex subunits in *D. discoideum* – in SWIP null cells, the distribution of WASH and strumpellin becomes cytosolic. This has led some researchers to claim that SWIP might provide an important anchor for the WASH complex or at least aid in recruiting such an anchor (Park et al., 2013). As SWIP is repeatedly found in large-scale ubiquitination screens (Stes et al., 2014; Thompson et al., 2014), it could be associated with the ubiquitination system recently linked to the WASH complex (Hao et al., 2013).

1. 4. 4. CCDC53

Coiled-coil domain containing protein 53 is, with its 194 amino acids, by far the smallest and also the least explored component of the WASH complex (Derivery et al., 2009). The only hint to its function is the similarity between the coiled-coil of CCDC53 and HSPC300, which is an analogous subunit of the WAVE complex (Jia et al., 2010); however, HSPC300 is almost as enigmatic as CCDC53 (Qurashi et al., 2007).

1. 5. FAM21

Human FAM21 is a 1,318 amino acids long protein with two distinct regions in its sequence: a short N-terminal globular domain which binds to other complex members, and a very long unstructured C-terminal “tail” domain (Jia et al., 2012) (**Figure 2**). This overall organization is conserved in other species – FAM21 is currently known to have homologues in all metazoans

(Derivery and Gautreau, 2010a), but also in more distant relatives including certain plant species (rice - *Oryza*), the slime mold *Dictyostelium* and other unicellular eukaryotes, but not fungi (Derivery and Gautreau, 2010a; Insall, 2013). There are four FAM21 genes in the human genome (FAM21A, FAM21B, FAM21C, and FAM21D), identical along most of their sequence. FAM21D is an exception as it is N-terminally truncated (Gomez and Billadeau, 2009). The letter coding of FAM21 genes is generally omitted in relevant publications and deciphering each gene's particular properties is currently impossible.

Figure 2 – Distribution of LFa motifs in the protein sequence of human FAM21. Black arrows indicate location of 21 LFa motifs in the C-terminal tail domain. Color shading of the molecule represents a similarity score between human and chicken FAM21 homologues. Adapted from Seaman et al., 2013.

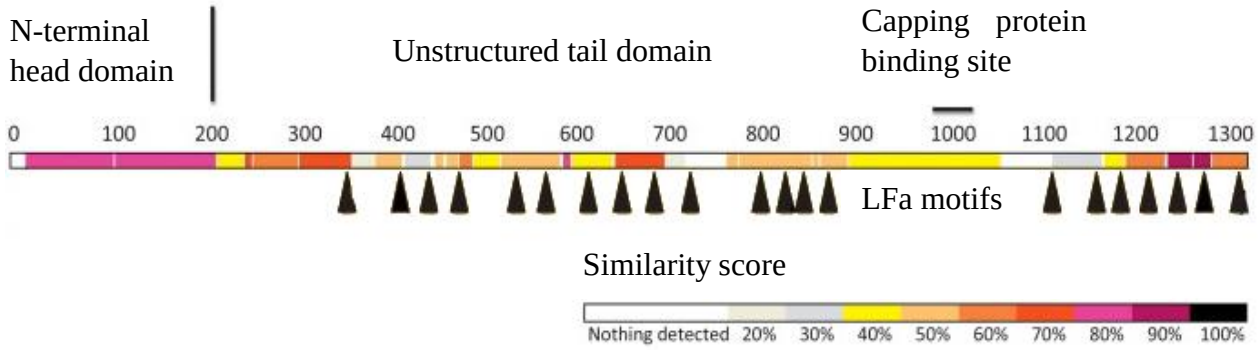

Discovery of unique sequence motifs in its C-terminal region (LFa motifs) was a major milestone in FAM21 research. It was simultaneously shown that these LFa motifs interact with a so-called retromer complex (Jia et al., 2012). New interaction partners have recently been published by various research groups (Hao et al., 2013; Phillips-Krawczak et al., 2015; Ryder et al., 2013). Six years after the discovery of the WASH complex, these findings call for a re-evaluation of its function. The following chapters will summarize the current state of knowledge on the cellular localization of FAM21 and the published interaction partners of FAM21 (or the WASH complex as a whole) with important conceptual consequences.

1. 5. 1. FAM21 localization

According to the mainstream scientific understanding, FAM21 is present in cells in a tight association with the rest of the WASH complex and thus usually localizes to places where the rest of WASH complex components are (Jia et al., 2010). However, FAM21 has been suggested to play a partially independent role in the final step of vesicle maturation in *Dictyostelium* (Park et al., 2013) and there are also reports of non-WASH complex FAM21 in the nucleus (Deng et al., 2014). In human cell lines, endosomal FAM21 shows high colocalization with other WASH complex components (Jia et al., 2010) and microscopic data acquired with one of the WASH complex components can be extrapolated to the other subunits of the complex.

First reports of WASH described a cytosolic distribution with certain enrichment in lamellipodia (Linardopoulou et al., 2007); these results can be attributed to extreme overexpression of WASH-GFP in cells. Recent articles consistently place WASH, together with FAM21 and other WASH complex components, onto the surface of endosomes and/or lysosomes (Derivery et al., 2009; Harbour et al., 2012; Park et al., 2013), but studies on nuclear FAM21 and WASH complex at the cell membrane have emerged recently (Deng et al., 2014; Hänisch et al., 2010).

In the human body, FAM21 is expressed ubiquitously but differentially; highest expression is found in the immune system (bone marrow, lymph node and spleen), linings of the digestive tract and ovaries. This expression pattern correlates fairly well with that of WASH and SWIP (data from Expression Atlas, Petryszak et al., 2014).

1. 5. 2. FAM21 on endosomes

According to immunofluorescence images acquired using anti-FAM21 antibody, a major pool of FAM21 displays an endosomal subcellular localization (Gomez and Billadeau, 2009). An enrichment on endosomes is also seen in *Dictyostelium* cells (Park et al., 2013). The localization pattern thus seems evolutionarily conserved.

Moreover, FAM21 is thought to be a direct anchor responsible for binding of the whole WASH complex to the endosomes (**Figure 3**). This is purpotedly achieved by binding to the retromer complex component Vps35 (Harbour et al., 2012; Helfer et al., 2013). How retromer is associated with membranes is largely unknown. Its sorting nexin (SNX) subunits 1, 2, 5 or 6 are usually held responsible for this thanks to their membrane-binding PX (phox) and BAR (Bin-Amphiphysin-Rvs) domains. Additionally, Rab7 and SNX3 play an important role in

recruiting the retromer to membranes (Harrison et al., 2014; Harterink et al., 2011; Rojas et al., 2007). Current prevailing dogma is that membrane-associated WASH complex is always bound to retromer. There are indeed studies indicating that WASH complex can exist on the membrane independently of retromer (Park et al., 2013; Ryder et al., 2013) and alternative models have been discussed. Using a PIP-strip overlay assay, FAM21 was shown to bind most phosphatidylinositol species as well as phosphatidylserine (Jia et al., 2010). Nevertheless, studies of FAM21 binding to membrane now usually concentrate on FAM21-retromer interaction (McGough et al., 2014a; Zavodszky et al., 2014), which is thought to be mediated by LFa motifs (Jia et al., 2012) present in the FAM21 C-terminal unstructured domain.

Figure 3 – WASH complex in association with the actin-coated endosomal membrane and its currently recognized interaction partners. WASH complex interacts with the retromer via FAM21 C-terminal domain binding to Vps35. Additional binding partners of WASH complex (Arp2/3, FKBP15, CP, CCC complex) and retromer (Rab7, SNX3) are shown. Adapted from Seaman et al, 2013 and Phillips-Krawczak et al., 2015.

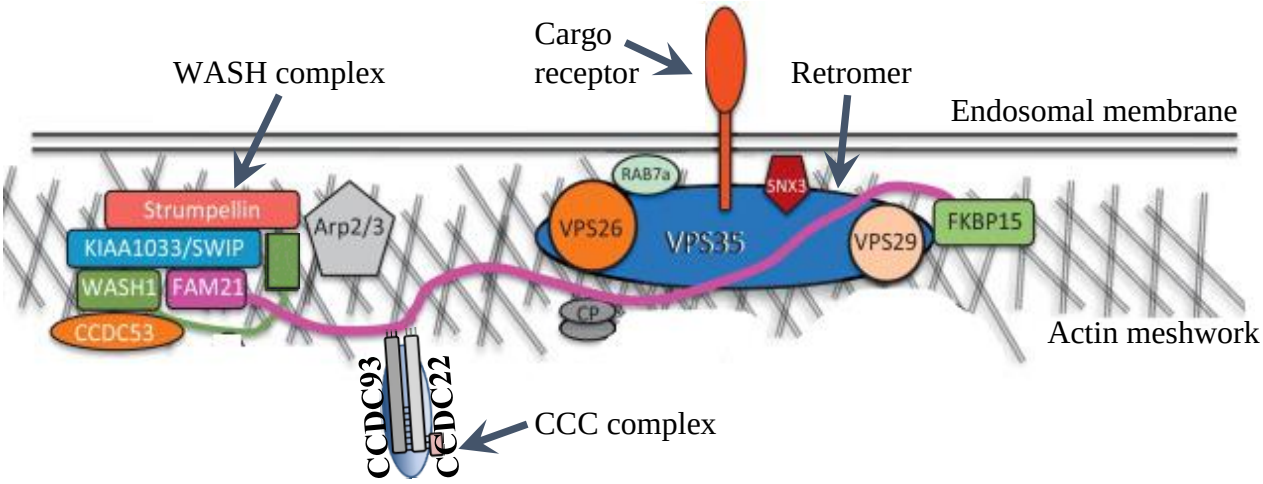

The nature of the vesicular membrane microdomain to which the WASH complex is attached is not completely clear. WASH localizes to vesicles which have EEA1-positive domains, meaning that it associates with early endosomes (of which EEA1 is a marker). However, the actual colocalization of WASH and EEA1 is found to be very low whenever sufficient microscope resolution is achieved (Gomez and Billadeau, 2009). It seems that WASH complex localizes to specific membrane domains of poorly defined nature. These domains are known to be enriched in retromer components SNX1 and SNX2 and represent the tubules emanating from

early endosomes in the process of retromer-dependent endosomal sorting (Gomez and Billadeau, 2009; Rowland et al., 2014). There may be additional markers of these microdomains such as Rab proteins Rab5, Rab4 and Rab11 – all were shown to colocalize with WASH on low-resolution microscopy images when overexpressed (Derivery et al., 2009). This is not surprising because all three above-mentioned Rab proteins localize to early and recycling endosomes (de Renzis et al., 2002). Rather, the poor resolution of the above-mentioned images does not allow dissection of captured early endosomes into specific membrane domains.

Presence of the WASH complex in other endosomal compartments is somewhat controversial. WASH does not colocalize with LAMP1 (a marker of lysosomes) according to some (Gomez and Billadeau, 2009), or colocalizes weakly but that is explained by a normal flux or maturation of vesicles (Gomez et al., 2012). Other studies report LAMP1-positive WASH-coated vesicles, as well as Rab7-positive WASH-coated vesicles, representing WASH-decorated lysosomes and late endosomes, respectively (Derivery et al., 2009). WASH complex indeed promotes recycling of membrane type 1 matrix metalloproteinase (MT1-MMP) from late endosomes to the cell surface (Monteiro et al., 2013). Lysosomal system collapses in WASH knock-out fibroblasts, suggesting at least a strong functional, if not physical relationship (Gomez et al., 2012).

More information is available for the lysosomal WASH complex in *D. discoideum*. This is attributed to the fact that *D. discoideum* constantly consumes material by endocytosis and phagocytosis (and sends it into the degradation pathway), while mammalian cell lines mainly use vesicular traffic for signalling-related recycling which occurs in the early endosomal compartment (Insall, 2013). It was reported that WASH complex drives V-ATPase recycling from lysosomes (Carnell et al., 2011). Most importantly, FAM21 is a regulator of this WASH-dependent lysosomal recycling and binds to the WASH complex only after the V-ATPase recycling step has occurred. Thereafter, FAM21 binds and promotes formation of WASH-positive "recycling" endosomes through which the WASH complex leaves the postlysosomes. In the absence of FAM21, the rest of the WASH complex accumulates on postlysosomes and hyperactivates the actin assembly on vesicles, leading to large perivesicular patches of polymerized actin (King et al., 2013; Park et al., 2013). Parallels to WASH-carrying recycling vesicles in mammals are unknown but worth exploring.

1. 5. 3. FAM21 at the plasma membrane

Reports of WASH complex at the cell membrane are scarce and usually left unmentioned in reviews. However, cell surface WASH complex, including its component FAM21, is crucial to understanding several WASH-dependent events. WASH complex localizes to the cell membrane at invadopodia, which correspond to regions where WASH-dependent recycling tubules (containing MT1-MMP) from late endosomes connect to the plasma membrane (Monteiro et al., 2013). A systematic study of WASH or FAM21 pool at the cell membrane is missing.

WASH complex and its components were also shown to be important for pathogen entry. Interestingly, FAM21 was originally identified as "Vaccinia Penetration Factor" (VEPF) because it is required for the entry of vaccinia virus (Poxviridae) into host cells. Using anti-FAM21 antibody, authors of the study demonstrated that FAM21 localized to plasma membrane microdomains (Huang et al., 2008). WASH (presumably in a complex with other WASH complex components) also localizes to the entry sites of *Salmonella* bacteria whose invasivity is reduced upon WASH knock-down (Hänisch et al., 2010).

1. 5. 4. FAM21 in the nucleus

First article on nuclear-localized FAM21 was published in 2014 (Deng et al., 2014) but such discovery should not be considered too surprising. Many actin-binding proteins had already been found in the nucleus before, including actin-related proteins (Arp), WASP, WAVE, actinin, filamin, several spectrins and myosins, gelsolin, profilin and cofilin (Castano et al., 2010). Actin is also detectable in the nucleus, predominantly in nucleolus and decondensed chromatin, and assembles into short polymers which do not bind phalloidin (Castano et al., 2010; Dingová et al., 2009).

Import of FAM21 into the nucleus is mediated by a nuclear localization sequence (NLS) and FAM21 also has a nuclear export sequence (NES). It accumulates in nucleus following inhibition of nuclear export using leptomycin B (Deng et al., 2014). The results are waiting for confirmation by other groups.

1. 6. Interaction partners of FAM21

Functional aspects of FAM21 will be discussed in this chapter. Because the physiological role of FAM21 in the cell cannot be fully explained without the proteins associated with it, the function will be discussed in terms of each interaction partner. To date, several direct interaction

partners were published, and many more indirect partners, which are recruited to one of the components of the WASH complex or the vesicular retromer-WASH supercomplex (**Figure 3**). The direct interaction partners include the other WASH complex components (Jia et al., 2010), capping protein (CP) subunits CapZα and CapZβ (Jia et al., 2010), vacuolar protein sorting-associated protein 35 [Vps35] (Harbour et al., 2012; Jia et al., 2012), FK506-binding protein 15 [FKBP15] (Harbour et al., 2012), receptor-mediated endocytosis-8 [RME-8] (Freeman et al., 2014) and coiled-coil domain containing protein 22 [CCDC22] and 93 [CCDC93] (Harbour et al., 2012; Phillips-Krawczak et al., 2015).

1. 6. 1. WASH complex components

Using yeast two-hybrid system, FAM21 was shown to directly bind to WASH and SWIP via its N-terminal 200 amino acids (Harbour et al., 2012). The other WASH complex components interact with FAM21 indirectly: yeast two-hybrid assays demonstrate that strumpellin binds to SWIP (Harbour et al., 2012) and CCDC53 is probably incorporated into the WASH complex via protein WASH, at least in *Caenorhabditis elegans* (Li et al., 2004). A 3D structure of the WASH complex is not available, electron microscopy analysis shows an approximately S- or Z-shaped protein with dimensions of approximately 10 × 20 nm (Jia et al., 2010).

Past studies were able to assign functions to some of the components of the WASH complex. Actin and Arp2/3 complex binding is accomplished through the C-terminal domain of WASH. This domain contains the so-called VCA (Verprolin – Connector – Acidic) module, showing strong homology to other WASP family members (Linardopoulou et al., 2007). WASH alone itself is highly active in stimulating actin polymerization; the constitutive (in)activity of the WASH complex is still questioned and the activation might be purely mediated by the recruitment to the membranes (Derivery and Gautreau, 2010b; Jia et al., 2010; Linardopoulou et al., 2007). Nevertheless, the immense importance of WASH is observed in the corresponding knock-out cell lines in which the actin patches and Arp2/3 are completely lost from early endosomes (Gomez et al., 2012). With the exception of FAM21, the role of the other WASH complex components is largely unknown (Derivery and Gautreau, 2010a; Freeman et al., 2013; Jia et al., 2010).

Some authors consider the capping protein (CP, a heterodimer of CapZα and CapZβ proteins) to be an integral component of the WASH complex, increasing the number of WASH complex polypeptide components to seven (Derivery and Gautreau, 2010a). The proportion of the pentameric to the "heptameric" WASH complex is a matter of scientific debate (Park et al.,

2013). Capping protein is associated with the WASH complex via FAM21 whose C-terminal tail contains a CP-binding consensus motif (Jia et al., 2010). CP itself is a well-known actin polymerization regulator which binds to the barbed end of actin filaments; every regulation of CP effectively affects actin polymerization (for review see Edwards et al., 2014). Capping protein was assigned a very important function in *D. discoideum*: when the WASH-mediated actin polymerization on vesicles is complete, FAM21 binds to this actin via CP. Such interaction leads to FAM21 recycling from the postlysosomal membrane (Park et al., 2013). This phenomenon has not been documented in mammalian systems yet.

1. 6. 2. Retromer

For years, WASH complex has been known to localize to retromer-enriched domains of early endosomes (Gomez and Billadeau, 2009). These membrane compartments serve as busy sorting stations which deliver cargo from the early endosomes towards plasma membrane or the Golgi apparatus, thus saving it from the degradative lysosomal pathway (for review see Jovic et al., 2010). Retromer consists of two main parts, the cargo-selective complex (a heterotrimer of Vps35, Vps29 and Vps26) and the sorting nexin (SNX) portion. Generally, one SNX5 or SNX6 dimerizes with one SNX1 or SNX2 sorting nexin to form the SNX portion of the retromer but additional sorting nexins (SNX3, SNX27) have been found to bind the complex as well. Retromer is an important machinery governing the endosomal cargo recycling and retrograde transport (for review see Burd and Cullen, 2014; Cullen and Korswagen, 2012).

Soon after the discovery of the WASH complex, a direct interaction between FAM21 and Vps35 was described, using co-immunoprecipitation as well as native immunoprecipitation followed by liquid chromatography-mass spectrometry (LC-MS/MS). To prove that the interaction between FAM21 and Vps35 is direct, a yeast two-hybrid system was employed. Vps35, used as a bait, readily detected FAM21, but when it was used as a prey, no such interaction was found (Harbour et al., 2010). The experiments were later extended to demonstrate that Vps35 binds to the C-terminal tail of FAM21, using native immunoprecipitation/MS, although not in the standard buffer system (Harbour et al., 2012).

Human FAM21 was later shown to include 21 copies of a novel LFa (leucine-phenylalanine-acidic) motif (**Figure 2**), which bind retromer Vps35 protein in a cooperative way. The typical sequence is L-F-$[D/E]_{3-10}$-L-F but deviations from the consensus motif are frequently seen (Jia et al., 2012). These motifs are evolutionary conserved and corresponding sequence patterns are present in *D. discoideum* (Insall, 2013). Endosomal

localization of the WASH complex was shown to depend on retromer using a knock-down approach (Harbour et al., 2010) and indirectly via overexpression of a C-terminal fragment of FAM21 that is able to displace the full-length FAM21 from endosomes. This displacing ability of the FAM21 fragment can be diminished by point mutations introduced into its sequence (Helfer et al., 2013).

Certain point mutations in Vps35 can also abrogate the binding of the WASH complex. Importantly, one of these point mutations is also seen in a subset of patients with a hereditary form of Parkinson disease, suggesting that the impairment of WASH complex-retromer interaction has pathological consequences in the human brain. Two recently published papers explored whether point mutation-disrupted Vps35-FAM21 interaction impairs endosomal localization of FAM21. They come to opposite conclusions - one of them confirms previous observations (Zavodszky et al., 2014), the other observes no change in FAM21 endosomal localization (McGough et al., 2014a). The question of whether retromer is the (only) receptor of the WASH complex at endosomes remains open.

A certain interaction between Vps35 and FAM21 is very probable, though, and functional explanations for such interaction were proposed. According to one of them, FAM21, with its 21 LFa motifs, may serve as a multivalent recruiting hub for arrays of retromer that form on the surface of endosomes (Jia et al., 2012). Such retromer-coated membrane domains would then function as recycling stations.

1. 6. 3. CCDC22 and CCDC93

Coiled-coil domain-containing proteins 22 and 93 (CCDC22, CCDC93) are proteins with poorly defined function (Schou et al., 2014), which were co-immunoprecipitated with FAM21 but not with Vps35, suggesting that they could be binding partners of a FAM21 subpopulation which is not retromer-associated (Harbour et al., 2012). It was then demonstrated that CCDC22 binds copper metabolism Murr1-domain containing (COMMD) proteins and increases degradation of IκB, thus promoting NF-κB signalling (Starokadomskyy et al., 2013). COMMD proteins are important regulators of cullin-RING (Really interesting new gene) ubiquitin ligases which in turn regulate NF-κB signalling (Maine et al., 2007; Mao et al., 2011).

Recently, CCDC22 and CCDC93 were found to form a complex with COMMD1 and a previously uncharacterized protein C16orf62 (UPF0505). This “CCC complex” binds FAM21 via the C-terminal ends of CCDC22 and CCDC93 subunits and regulates the trafficking of the

ATP7A receptor in human cell lines (Phillips-Krawczak et al., 2015), possibly through the WASH complex as a whole.

1. 6. 4. FKBP15

FK506-binding protein 15 (FKBP15, also known as WAFL) is a WASP homology domain-containing protein with a prolyl-isomerase domain which can be bound by an immunosuppressive drug FK506. It was first identified as a retromer-interacting protein which loses its endosomal localization upon knock-down of retromer components Vps26 or Vps35 (Harbour et al., 2010). FKBP15 binds to the FAM21 tail and knock-down of FAM21 causes reduced endosomal localization of FKBP15 (Harbour et al., 2012; Jia et al., 2012). Interaction of FKBP15 with the WASH complex is independent of the retromer according to a recent publication (Zavodszky et al., 2014). The specific role of FKBP15 remains elusive.

1. 6. 5. RME-8

Receptor-mediated endocytosis-8 (RME-8) is a phosphatidylinositol-3-phosphate (PI(3)P)-binding protein (Xhabija et al., 2011) of the DNAJ family that has recently been identified to interact with the C-terminal tail of FAM21 (Freeman et al., 2014). Interaction with the WASH complex is not needed for the membrane association of RME-8, as shown by knock-down experiments of individual WASH complex components. Specific function of RME-8 is currently unknown, but silencing of RME-8 causes pronounced membrane tubularization of endosomes, and shift of several endosomal proteins from the "central" endosomal body to the sorting nexin-1 (SNX1)-decorated emanating tubules. However, SNX1, a retromer component, is disposable for the membrane association of RME-8 (Freeman et al., 2014).

1. 6. 6. SNX27

It was already mentioned in the preceding chapters that the cargo-selective complex of the retromer associates with sorting nexins. Among those, sorting nexin 27 (SNX27) has the strongest affinity towards WASH complex components, as shown from co-immunoprecipitation experiments (Steinberg et al., 2013). GFP trap-based immunoprecipitation of SNX27 domains shows SNX27 possesses three distinct modules binding to (1) the cargo-selective complex, (2) the WASH complex and (3) the SNX-BAR domain of "classical" sorting nexins. The SNX27-WASH complex interaction is not mediated via retromer because SNX27 co-immunoprecipitates with FAM21 N-terminal globular domain,

even though this domain cannot co-immunoprecipitate with retromer. Thus, SNX27 associates with the WASH complex directly, but the exact nature of this interaction is unknown (Steinberg et al., 2013; Temkin et al., 2011) and it is not a confirmed FAM21-interacting protein at the moment.

2. Goals

Careful review of the literature revealed a wide array of known and suspected interaction partners as well as a diverse set of cellular locations, where WASH complex (and specifically FAM21) localizes. We hypothesized that early endosomal interactome cannot fully explain the function of the WASH complex because its components localize to other places in the cell. To shed more light on localization and interaction partners of FAM21, a key WASH complex component with an unusual motif in its primary structure, we decided to:

1. Determine the subcellular localization of FAM21.
2. Uncover novel interaction partners of FAM21 and confirm those currently known.
3. Disclose the proteins binding to LFa motifs

3. Experimental procedures

3. 1. Materials

If not stated otherwise, the chemicals and reagents were purchased from Sigma-Aldrich (USA).

3. 1. 1. Media and buffer solutions

Lysogeny broth [LB]

For 1 L of LB:

- 10 g bacto tryptone (Becton, Dickinson and Co., France)
- 5 g yeast extract (AppliChem, Germany)
- 10 g sodium chloride (NaCl)

Adjusted to pH 7.4, autoclaved.

Super optimal broth (SOB)

For 1 L of SOB:

- 20 g bacto tryptone
- 5 g yeast extract
- 0.5 g sodium chloride (NaCl)
- 2.5 mL of 1M potassium chloride (KCl)

Adjusted to pH 7, autoclaved, supplemented with 20 mL of 1 M glucose before use.

HL5 medium

For 1 L of HL5:

- 14 g peptone
- 13.5 g glucose
- 7 g yeast extract
- 0.5 g disodium phosphate (Na_2HPO_4)
- 0.5 g monopotassium phosphate (KH_2PO_4)

Adjusted to pH 6.5, autoclaved.

Mammalian cell growth medium

- Dulbecco's Modified Eagle Medium (DMEM) with GlutaMAX-I, 4.5 g/L D-glucose and pyruvate (Life Technologies)
- 10% fetal bovine serum (Gibco, USA), inactivated and filtered through 0.2 μm antibacterial filter
- 1% penicillin/streptomycin 100X solution (PAA Laboratories, Austria)

1X Laemmli buffer

- 15.6 mM TRIS-hydrochloride pH 6.8 (Roth, Germany)
- 0.5% sodium dodecyl sulfate (SDS)
- 2.5% glycerol (Lachema, Czech Republic)
- trace amounts of bromophenol blue (Serva, Germany)

Supplied with 0.1 M dithiothreitol (DTT) before use.

8% separating polyacrylamide gel

- 0.375 M Tris (pH 8.8)
- 27% (v/v) acryl-bisacryl mix (Serva, Germany)

- 1% SDS
- 1% ammonium persulfate
- water to 10 mL
- 0.04% tetramethylethylenediamine (TEMED)

5% stacking polyacrylamide gel

- 0.125 M Tris (pH 6.8)
- 5% (v/v) acryl-bisacryl mix
- 1% SDS
- 1% ammonium persulfate
- water added to 4 mL
- 0.1% TEMED

Running buffer

- 25 mM TRIS base
- 192 mM glycine
- 0.1% SDS

Filtered before use.

Blotting buffer

- 25 mM TRIS base
- 192 mM glycine
- 20% methanol (Penta, Czech Republic)

Filtered before use.

Phosphate buffer saline [PBS]

- 137 mM sodium chloride (NaCl)
- 2.7 mM potassium chloride (KCl)
- 10 mM disodium phosphate (Na_2HPO_4)
- 1.8 mM monopotassium phosphate (KH_2PO_4)

Premixed as 10X solution, filtered and adjusted to pH 7.4.

Hank's Buffered Salt Solution [HBSS]

- 137 mM sodium chloride (NaCl)
- 5 mM potassium chloride (KCl)
- 1.1 mM disodium phosphate (Na_2HPO_4)
- 0.4 mM monopotassium phosphate (KH_2PO_4)
- 5.5 mM glucose
- 4 mM sodium bicarbonate ($NaHCO_3$)

Autoclaved.

Microtubule stabilizing buffer [MSB]

- 20 mM 2-(N-morpholino)ethanesulfonic acid (MES)
- 2 mM ethylene glycol tetraacetic acid (EGTA)
- 2 mM magnesium chloride ($MgCl_2$)
- 4% (w/v) polyethylene glycol 6000 (PEG)

Dissolved in HBSS.

Electroporation Buffer [EB]

- 5 mM disodium phosphate (Na_2HPO_4)
- 5 mM monopotassium phosphate (KH_2PO_4)
- 50 mM sucrose

Adjusted to pH 6.5.

TAE buffer

- 40 mM Tris pH 8.0
- 20 mM acetic acid (Penta, Czech Republic)
- 1 mM ethylenediaminetetraacetic acid (EDTA)

Bacterial lysis buffer

- 1% Tx-100
- 20 mM dithiothreitol

Dissolved in PBS and kept at 4 °C, supplemented with 1X HALT cocktail (Thermo Scientific, USA) before use.

TNE buffer

- 50 mM Tris–HCl (pH 7.4)
- 100 mM NaCl
- 0.1 mM EDTA

KK2 phosphate buffer (pH 6.2)

- 16.5 mM monopotassium phosphate (KH_2PO_4)
- 3.8 mM dipotassium phosphate (K_2HPO_4)

3X lysis/crosslinking buffer

- 60 mM HEPES (4-(2-hydroxyethyl)-1-piperazine ethanesulfonic acid) pH 7.4
- 6 mM magnesium chloride ($MgCl_2$)
- 9% UltraPure formaldehyde (Polysciences, United Kingdom)
- 0.6% Triton X-100
- 1X Halt Protease Inhibitors (Thermo Scientific, USA)

Washing buffer A

- 0.2 M Tris-HCl (pH 8.0)
- 0.1% Triton X-100
- 1X Halt Protease Inhibitors (Thermo Scientific, USA)

Washing buffer B

- 50 mM HEPES (pH 7.4)
- 2 mM magnesium chloride ($MgCl_2$)
- 0.1% Triton X-100
- 1X Halt Protease Inhibitors (Thermo Scientific, USA)

Washing buffer C

- 50 mM HEPES (pH 7.4)
- 2 mM magnesium chloride ($MgCl_2$)
- 1X Halt Protease Inhibitors (Thermo Scientific, USA)

Extraction buffer

- 50 mM Tris-HCl (pH 8.0)
- 150 mM sodium chloride (NaCl)
- 1% Triton X-100
- 1% sodium deoxycholate
- 0.3% SDS
- 5 mM EDTA

- 4 mM dithiothreitol (DTT)
- 1X Halt Protease Inhibitors (Thermo Scientific, USA)

Pulldown washing buffer

- 50 mM Tris-HCl (pH 8.0)
- 150 mM sodium chloride
- 5 mM EDTA
- 1X Halt Protease Inhibitors (Thermo Scientific, USA)

3. 1. 2. Antibodies

Primary and secondary antibodies used in the experiments are summarized in **Table 1** and **Table 2**, respectively.

Table 1: Primary antibodies

Specificity	Monoclonal/ polyclonal	Species	Manufacturer	Cat. no.	Dilution for IMF	Dilution for WB
LAMP1 (D2D11)	Monoclonal	Rabbit	Cell Signaling	9091	1:300	-
Rab7 (D5F2)	Monoclonal	Rabbit	Cell Signaling	9367	1:300	-
EEA1 (C45B10)	Monoclonal	Rabbit	Cell Signaling	3288	1:500	-
Golgin97	Monoclonal	Mouse	Molecular Probes	A21270	1:400	-
FAM21 A-D (S-13)	Polyclonal	Rabbit	Santa Cruz	137995	1:100	-
GFP	Polyclonal	Rabbit	Abcam	290	-	1:2000
c-Myc	Monoclonal	Mouse	Exbio	11-433-C100	1:500	1:1000

Table 2: Secondary antibodies

Trade name	Manufacturer, cat. no.	Dilution for IMF	Dilution for WB
Cy5-conjugated AffiniPure Donkey Anti-Rabbit IgG (H+L)	Jackson Immunoresearch, 711-175-152	1:500	-
Cy3-conjugated AffiniPure Goat Anti-Mouse IgG (H+L)	Jackson Immunoresearch, 115-165-146	1:500	-
Rabbit anti-Goat IgG (H+L) Secondary Antibody, Alexa Fluor 488 conjugate	Molecular Probes, A11078	1:400	-
Peroxidase-conjugated AffiniPure Goat Anti-mouse IgG (H+L)	Jackson Immunoresearch. 115-035-146	-	1:10,000

3. 1. 3. Constructs

Vectors pEGFP-mWASH, pEGFP-FAM21 were a generous gift from M. Seaman, vector pEGFP-Rab11 was a gift from V. Žíla, vector pCS2 hHRS-RFP was donated by Edward De Robertis. Mouse WASH (mWASH) was cloned into pEGFP-C1-3, FAM21 into pEGFP-N1-3, Hrs into pCS2-C-HA-RFP vector, as described in original publications (Choudhury et al., 2002; Harbour et al., 2010; Taelman et al., 2010).

FAM21-myc-his expression vector was prepared by T. Brabec via PCR amplification from HeLa cDNA, ligation into pJET cloning vector and subcloning into pcDNA 4.0. *Dictyostelium* expression vectors were provided by P. Thomason; FAM21 had been cloned into pDM448, creating a N-terminal GFP tag (Park et al., 2013), MROH1 (Maestro Heat-Like Repeat Family Member 1) had similarly been cloned into pDM450 to produce a C-terminally tagged MROH1-GFP (unpublished). Preparation of GST [glutathione-S-transferase]-tagged FAM21 fragment constructs is described in the text.

Plasmid DNA was isolated using plasmid DNA miniprep kit "Nucleospin" (Macherey-Nagel, Germany) from the overnight culture of 4 mL LB medium containing the appropriate antibiotic and inoculated with the appropriate DH5α bacterial strain. Concentration of the DNA was determined with Nanodrop ND-1000.

3. 2. Human cell line experiments

3. 2. 1. Cell culture

All experiments in human cells were conducted using U2OS osteosarcoma cell line. These were cultivated at 37 °C / 4% CO_2 atmosphere. Tissue culture flasks 25 cm^2 (TPP, Switzerland) with 8 mL of the mammalian cell growth medium were used for long-term cultivation unless otherwise noted. Cells were subcultured twice a week using 2.5 mL trypsin/EDTA solution (PAA Laboratories, Austria) and centrifugation at 150g/25 °C for 4 min. During a typical subculturing procedure, 1/10 of the cells was resuspended in 8 mL of fresh medium and transferred back into a new flask.

3. 2. 2. Transfection and pre-treatments

Cells were transiently transfected with plasmid DNA as follows. For subsequent proteomic analysis, cells were grown in 2 mL of DMEM with 7% fetal bovine serum using 6-well cell culture plates (TPP, Switzerland). When intended for microscopy, cells were similarly plated

on coverslips (Marienfeld, Germany; thickness 0.13-0.16 mm) in 6-well plates without the surface modification (Böttger, Germany). The coverslips were prewashed in hydrochloric acid and sterilized. In each case, an approximate cell density of 30% was desired for the day of transfection when for microscopy, 60% when for biochemistry. Cells were transfected with X-tremeGENE HP DNA Transfection Reagent (Roche, Germany) using standard procedure. Briefly, for transfection of each well in a 6-well plate, 1 μg of plasmid DNA was added to 100 μL of DMEM, 2 μL of the transfection reagent were added to another 100 μL of DMEM and subsequently mixed together. Following 15 min incubation the mixture was pipetted into the wells with medium and cells were grown at 37 °C / 4% CO_2 for 24 hours.

For siRNA experiments, cells were prepared as for DNA transfection and then transfected with 20 pmol of siRNA premixed in DMEM with 5 μL Lipofectamine RNAiMAX (Invitrogen, USA). Cells were then grown for 48 hours.

For internalization experiments, 5 μg of Alexa 594-conjugated transferrin (Life Technologies, USA) per well in a 6-well dish was added to the medium 2 hours prior to the fixation step (from a stock of 5 mg/mL in PBS). 0.5 μg of lipophilic tracer DiI (Invitrogen, USA) per well was added to the medium 3 hours prior to the fixation (from a stock of 1 mg/mL in DMSO).

To create a Rab11-GFP stable cell line, Rab11-GFP was expressed in U2OS cells and cultivated in the presence of 400 μg/mL G418 (PAA Laboratories, Austria) for 3 weeks.

3. 2. 3. SDS PAGE/Western blot

A simple proteomic analysis was performed using sodium dodecyl sulfate (SDS) polyacrylamide gel electrophoresis (SDS PAGE) followed by Western blot. Cells were harvested from 6-well dishes using trypsin/EDTA and subsequent centrifugation as described in section “Cell culture”, followed by washing in 1 mL of PBS and repeated centrifugation. Remaining PBS was carefully removed and the cells were resuspended in 100-150 μL of 1X Laemmli buffer. Cells were sonicated for 10 s, passed 5 times through a 26-gauge syringe needle (B. Braun, Germany), heated at 97 °C for 10 min, centrifuged for 20 min/4 °C/21,000g and the soluble fraction was then kept on ice or at -80 °C for long-term storage.

For SDS PAGE, 8% separating and 5% stacking polyacrylamide gels were casted in a gel caster (Labnet Enduro) and samples were separated for 1.5 hours at 120 Volts in running buffer. PAGE Ruler Plus Prestained Protein Ladder (Thermo Scientific, USA) was used as a protein ruler. The gel was then removed from the glasses and preincubated in a small amount of blotting

buffer (10 min). Proteins were transferred onto a nitrocellulose membrane (pore size 0.2 μm, GE Healthcare, Germany) using a wet sandwich system in blotting buffer at 4 °C/30 Volts overnight (to increase transfer of high molecular-size proteins).

3. 2. 4. Immunofluorescence

Cells grown on coverslips were fixed for 10 min in 3% paraformaldehyde (dissolved in microtubule stabilizing buffer [MSB]) which was kept in 10 mL aliquots at -20 °C and never stored for more than 5 months. For direct imaging, cells were washed three times for 5 min in MSB and then mounted onto microscope slides (Marienfeld, Germany) in a droplet of Prolong Gold Antifade Reagent (Invitrogen, USA) supplied with 4',6-diamidino-2-phenylindole (DAPI) as a nuclear stain.

For immunofluorescence, cells were permeabilized for 5 min in 0.1% Triton X-100 (Sigma-Aldrich, USA) in phosphate buffer saline (PBS), or in 0.1% Tween 20 (Sigma-Aldrich, USA) in PBS when membranes had been stained with DiI, according to a published protocol on handling DiI stained cells (Lukas et al., 1998). Subsequently, coverslips were washed three times in PBS (which was the standard washing protocol for the subsequent steps). Coverslips were then incubated for 45 min in a ~80 μL droplet of 3% bovine serum albumin (Roth, Germany) in PBS with an added primary antibody at desired dilution. When simultaneous staining with two primary antibodies was desired, cells were incubated in these antibodies consecutively and washed in PBS between the incubations. Similarly, when cells were stained with conjugated phalloidins (Alexa Fluor 488 Phalloidin, Alexa Fluor 657 Phalloidin; Invitrogen, USA), they were first incubated in primary antibody and then in phalloidin, or vice versa. Conjugated phalloidin (0.5 unit of the reagent per coverslip) was added in 3% BSA in PBS. Cells were then washed and incubated with desired secondary antibody in 3% BSA in PBS for 45 min. If several secondary antibodies were used in the setting, cells were incubated in all of them simultaneously.

After the last incubation step, coverslips were washed and then briefly immersed in deionized water to remove salts from the buffer solutions. Finally, they were mounted on microscope slides in a droplet of Prolong Gold and stored in dark at 4 °C at least overnight to cure properly.

3. 2. 5. Microscopy

All microscope slides were first observed on Olympus Cell^{R} epi-fluorescence microscope with a Hammatsu ORCA C4742-80-12AG camera and an UPLSAPO 60× objective with oil

immersion. Exposition time and gain of the camera were set to maximize the dynamic range of the image. Usually, single scans through the middle portion of the cells were acquired in all relevant channels of the fluorescence sample. Z-stacks per each 0.5 μm were sometimes used instead of single scans; these are accordingly marked in the result section. Images were exported as raw TIF files and assembled in ImageJ. When necessary for colocalization analysis, pixel shift corrections were used by translating corresponding channels relative to each other using a command "Translate…". For the purpose of this thesis, pictures or their insets were exported into Microsoft Word and brightness and contrast were enhanced.

Specificity of the signal was controlled using samples treated with only secondary antibody/antibodies as negative controls. In case several channels were acquired from one image, absence of bleed-through between colour channels was verified using single-stained samples. In some cases, absence of bleed-through between channels was verified using confocal microscopy (Leica TCS SP2).

Additionally, some images were acquired using Nikon N-SIM superresolution microscopy (structured illumination). This high-resolution system, built on Nikon Eclipse Ti, was equipped with CFI SR Apochromat TIRF 100× oil objectives (numerical aperture 1.49) and EMCCD camera iXon3 DU-897E. Images acquired through this system were reconstructed using software "NIS-Elements Ar V4.20" with N-SIM module. Pseudo-widefield images were generated for the sake of comparison using SIMCheck plugin in ImageJ.

To calculate puncta/image intensity ratios for association analysis, FAM21 channel was thresholded and puncta were annotated using command "Analyze particles" (**Figure 4A**). Each particle was saved as a region of interest (ROI, **Figure 4B**) and extended laterally by 0.25 μm using command "Make Band" (**Figure 4C**) as follows:

```
run("Analyze Particles...", "size=0-20 display add");
for (i=0; i<roiManager("Count"); i++) {
roiManager("Select", i);
run("Make Band...", "band=0.25");
roiManager("Update");
}
```

ROIs were then overlaid to the second channel (**Figure 4D**) and number of marker-associated ROIs was manually counted. For association analysis in Vps35 knockdown experiments, an automated approach was used. The intensity of the second channel inside the extended ROIs was compared to the average intensity of the image to calculate the puncta/image intensity ratio,

using command "Measure". Standard deviation using individual ROI measurements was calculated in Microsoft Excel.

Figure 4 – Puncta/cell intensity ratios determination. (**A**) Cropped portion of the FAM21 channel. (**B**) Thresholded image with FAM21 puncta. (**C**) FAM21 puncta extended laterally by 0.25 µm. (**D**) FAM21 extended puncta overlaid on EEA1 channel.

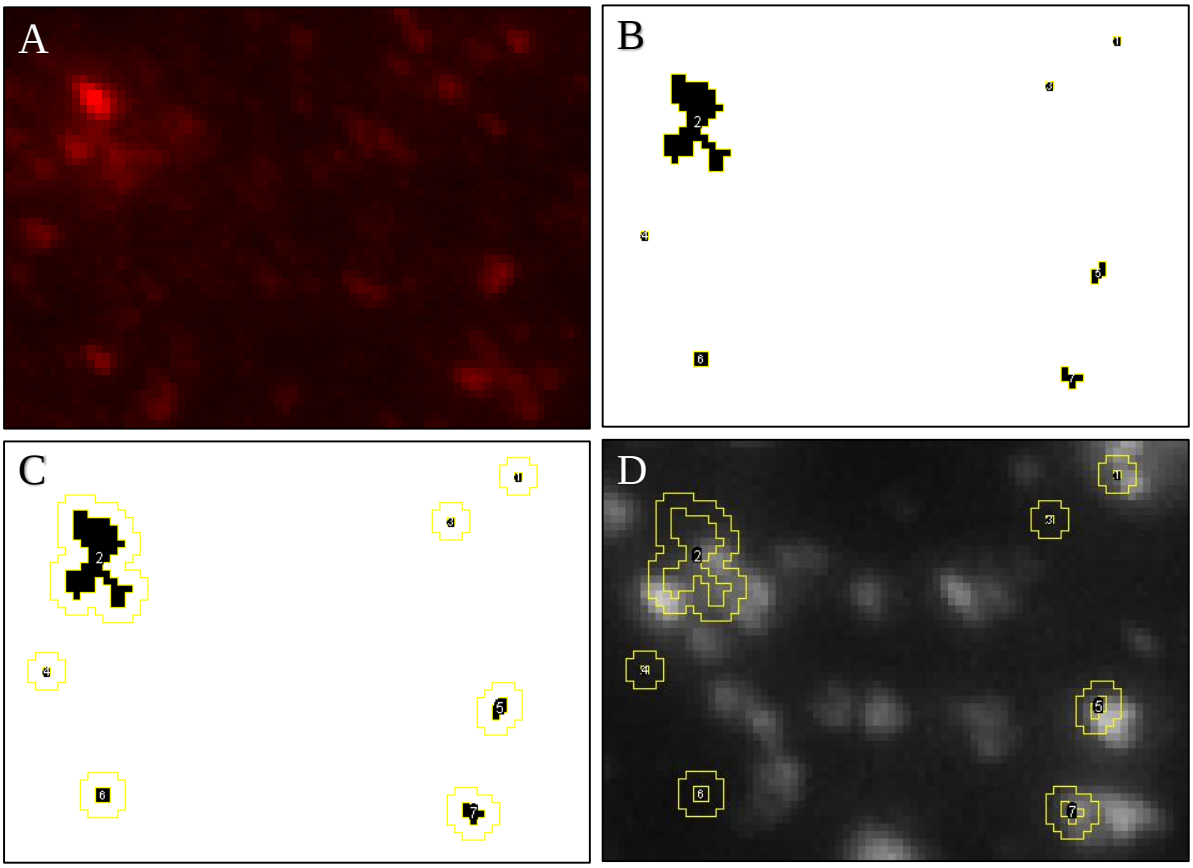

3. 2. 6. Quantitative PCR

Cells were grown to confluence and harvested by trypsinization and two rounds of washing in PBS. Total RNA was isolated using RNeasy Mini Kit (Qiagen, Germany), quality-checked by electrophoresis and transcribed into cDNA using SuperScript III Reverse Transcriptase (Life Technologies, USA). Standard manufacturer's instructions were followed. PCR reactions (total volume 20 µL) consisted of 10 µL SuperMix iTaq Universal SYBR Green Supermix (Biorad, USA), 5 µL cDNA pre-diluted 1:20, 0.5 µL of each primer and 4 µL deionized water. Samples in triplicates were pipetted into a 96-well plate and quantitative polymerase chain reaction

(qPCR) was executed in IQ-5 Multicolor RT PCR Detection System (Biorad, USA). Non-transcribed RNA was used as a control of cDNA quality, actin and glyceraldehyde 3-phosphate dehydrogenase (GAPDH) primers were used as standards.

3. 3. *Dictyostelium* experiments

3. 3. 1. Cloning

Primers for amplification of desired sequences were designed using the published genome of *Dictyostelium discoideum* and included EcoRI and XhoI restriction sites. PCR mix (25 μL) included 12.5 μL of PrimeSTAR Max mixture (Clontech, USA), 10 μL deionized water, 1 μL of each primer (10 μM working stocks) and 0.5 μL of template DNA solution. The PCR program consisted of 30 s of initial denaturation (98 °C), 20 amplification steps (10 s at 98 °C, 10 s at 55 °C, 20 s / kilobase at 68 °C) and final elongation step at 68 °C, 10 s. The product was mixed with 6X Orange loading dye solution (Fermentas, USA) and separated on 1% agarose gel electrophoresis in TAE buffer with O'GeneRuler 1kb DNA ladder (Fermentas, USA) as a ruler. Bands were checked against the DNA ladder and purified with a commercial gel extraction kit (Zymo Research, USA).

PCR fragments were first cloned into pCR-Blunt II-TOPO cloning vector using the Zero Blunt TOPO PCR Cloning Kit (Invitrogen, USA) and the recommended mixture composition and immediately transformed into competent DH5α bacteria using a heat-shock approach (bacteria melted on ice, ligation mixture added, incubation on ice for 30 min, heat-shock at 42 °C for 1 min, on ice for 10 min and shaking in 400 μL of SOC medium for 45 min). Bacteria were grown overnight at 37 °C on Lysogeny broth (LB) medium agar dishes with supplemented kanamycin. For plasmid miniprep, six colonies for each candidate bacterial strain were inoculated into 4 mL of LB supplemented with kanamycin and grown overnight at 37 °C. Vectors were checked by restriction digest (EcoRI and XhoI restriction endonucleases in EcoRI buffer, New England Biolabs, USA) and by sequencing.

To prepare GST-fused constructs, fragments of the insert from the digest were subcloned into an inducible pGEX-4T2 vector (GE Healthcare, Germany) using T4 ligase (Thermo Scientific, USA). The ligation mixture was then transformed into competent DH5α bacteria and these were grown overnight at 37 °C on ampicillin dishes. Colonies were screened by restriction digest.

3. 3. 2. *Dictyostelium* cell culture

D. discoideum axenic cell lines were grown in 10 mm Petri dishes in 20 mL of HL5 axenic liquid medium. Cells were cultivated at 22 °C and subcultured twice a week by vigorously washing the ~confluent cells with 10 mL of fresh HL5 medium and centrifuging at 340g for 3 minumintes in 15 mL falcon tubes. About 1/100 of cells was resuspended in fresh medium and transferred into a new Petri dish.

3. 3. 3. *Dictyostelium* transfection

Tagged genes were expressed in corresponding null cells (FAM21-null AX4, MROH1-null AX3) created by targeted gene disruption and provided by Robert Insall and Peter Thomason at Beatson Institute for Cancer Research, Glasgow. The null cells were kept under blasticidin resistance (10 μg/mL, Blasticidin S hydrochloride, Melford Labs, United Kingdom) to ensure that only knock-out cells are present.

GFP-tagged constructs of FAM21 and MROH1 were transfected into the appropriate null cell lines. First, cells were harvested as if for subculturing, washed in electroporation buffer (EB), centrifuged again, and resuspended in an appropriate volume of EB to achieve a density of $2x10^7$ cells/mL (counted with Casy counter). 1.5 μg of miniprep DNA was mixed with 420 μL of cell suspension in an ice-cold cuvette and electroporated using BTX electroporator at 500V (3 millisecond pulse). Immediately after that, cells were transferred to a Petri dish with HL5 medium and grown overnight. Hygromycin B (50 μg/mL, Life Technologies, United Kingdom) was added to the cells after overnight growth and surviving cells were grown to confluence. Expression of GFP-tagged proteins was checked by live cell confocal microscopy (Olympus FV1000) and by SDS PAGE/Western blot (using anti-GFP antibody, Abcam, United Kingdom).

Procedure for SDS PAGE and Western blot of *D. discoideum* samples was very similar to that employed for mammalian cell line samples with several small differences. Commercial 12% NuPAGE gels with 4% stacking gel and corresponding commercial buffers for SDS PAGE and Western blot were used (Life technologies, USA). PAGE Ruler Prestained Protein Ladder (Thermo Scientific, USA) was used as a protein ruler.

3. 3. 4. Crosslinking assay

A crosslinking-based assay for the study of protein-protein associations was employed (**Figure 5**). Cell lines expressing the GFP-tagged FAM21 and a control cell line expressing

GFP-tagged MROH1, an endosomal peripheral protein currently not known to associate with FAM21, were grown to confluence in two 14 mm dishes in 25 mL of HL5 medium. They were harvested as if for subculturing (see above) and cells from the duplicate dishes were pulled together, washed 3 times in KK2 phosphate buffer (pH 6.6), finally resuspended in 4 mL KK2 buffer. For the rest of the experimental procedure, samples were strictly kept on ice and all buffers were supplemented with protease inhibitors.

Figure 5 – Protocol used for the crosslinking assay of protein-protein associations.

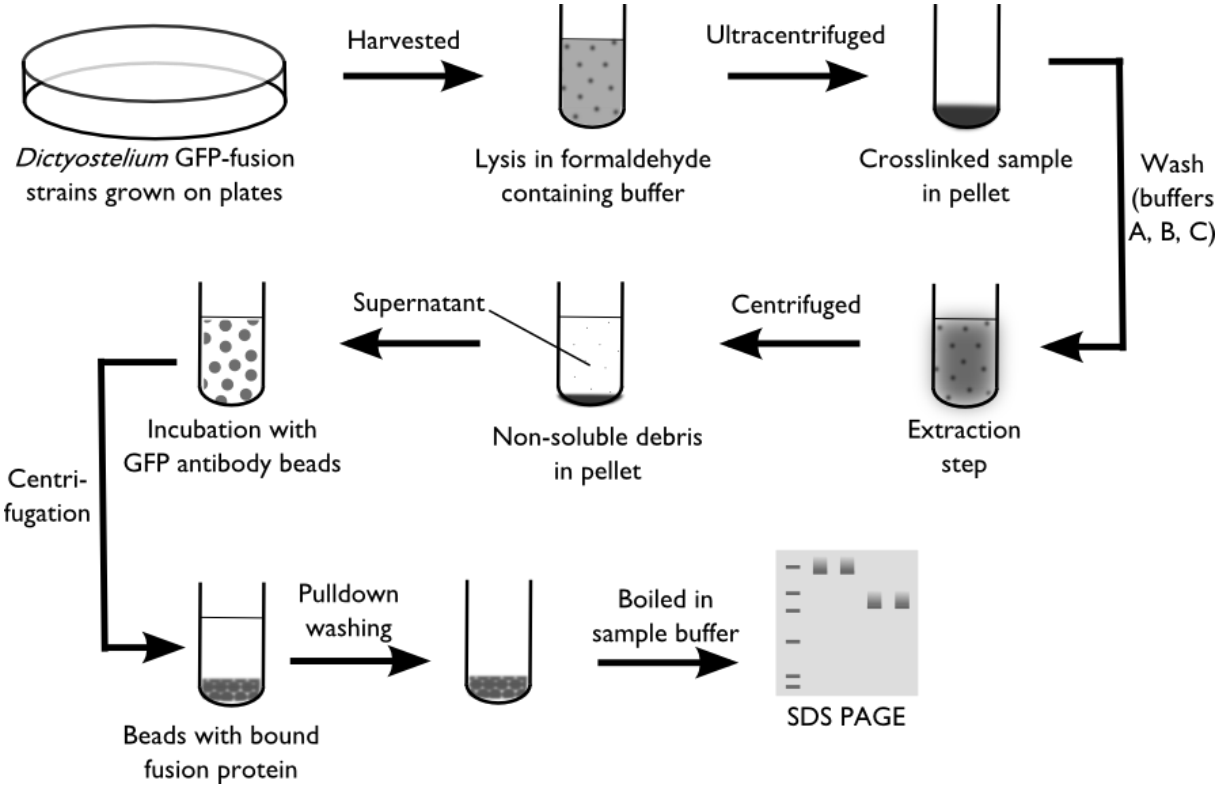

Each of the two samples was mixed with 2 mL of 3× lysis/crosslinking buffer which contained 9% formaldehyde. Samples were mixed by inverting and incubated for 5 min at 4 °C shaking. After quenching the samples with 6 mL ice-cold 1.75 M Tris-HCl buffer (pH 8.0), samples were centrifuged at 22,000g, 4 °C, 5 min. This was followed by three washing steps (in washing buffers A, B and C). The remaining pellet was then resuspended in 250 µL of extraction buffer and extraction was left to proceed for 40 min on a shaker. After a centrifugation step at 16,000g (4 min, 4 °C), the extract was collected and mixed with 250 µL of pulldown washing buffer containing 15 µL of prewashed GFP-Trap A beads (Chromotek, Germany). After incubation

for 2 hours, beads were spun down at 2,700g (for 2 min) and washed 3 times with pulldown washing buffer and once with Tris-HCl buffer (pH 8.0). Beads were then resuspended in 10 µL of 1.5% SDS, heated at 70 °C for 10 min and dissolved in 30 µL additional MilliQ water and NuPAGE sample buffer. Sample was then divided into two approx. 20 µL aliquots – one was heated at 70 °C for 8 min ("crosslinked sample"), the other was de-crosslinked at 100 °C for 25 min.

Samples were loaded on SDS PAGE as described above, and analysed by the mass spectrometry unit. There, the gel was reduced with dithiothreitol, alkylated with iodoacetamide, digested with trypsin and the resulting peptides were analysed on liquid chromatography-mass spectrometry (LC-MS/MS) in data-dependent analysis with Orbitrap Velos. Data were searched with Mascot and Maxquant against *D. discoideum* database and combined in Scaffold.

3. 3. 5. GST pulldown

Inducible vectors pGEX-4T2 bearing the desired GST-tagged fragments were transformed into competent BL21 or Rosetta2 bacterial strains, which were plated onto ampicillin dishes (or, in the case of Rosetta2 strain, ampicillin + chloramphenicol) and grown overnight. Three colonies of each were grown in 4 mL of LB medium overnight at 37 °C shaking. Next day, 3 mL of these bacterial growths were inoculated into two falcon tubes with 17 mL of fresh LB medium and grown for 1-2 hours at 37 °C. One of the falcon tubes was then supplemented with 0.5 mM isopropyl β-D-1-thiogalactopyranoside (IPTG, Sigma-Aldrich, USA) and bacteria were grown at 30 °C for 6 hours shaking, or 22 °C overnight (both approaches had comparable results). A 1 mL aliquot was then centrifuged at 4000g for 20 min, resuspended in bacterial lysis buffer, centrifuged at 37,000g for 30 min and the supernatant was boiled in NuPAGE sample buffer (Invitrogen, USA) at 100 °C for 10 min. Resulting "crude" bacterial lysates were then separated on SDS PAGE as described in the preceding section, stained with InstantBlue (Expedeon, United Kingdom) and visually checked for a band of an appropriate size, present in IPTG-induced samples and not in control non-induced cells. In samples where a hint of such band was detected, the rest of the bacterial sample (19 mL) was similarly processed but finally resuspended in 1 mL of bacterial lysis buffer and incubated with 8 µL of prewashed Amintra glutathione beads (Expedeon, United Kingdom) for at least 3 hours at 4 °C. Incubation was followed by boiling in NuPAGE sample buffer as described above, separation on a SDS PAGE gel and staining with InstantBlue.

When successful, a larger-scale culture (500 mL volume) was similarly cultivated overnight at room temperature shaking and induced with IPTG on the following morning. Bacteria were then grown for 6 hours at 30 °C shaking, centrifuged, resuspended in 25 mL of bacterial lysis buffer and sonicated 8 times for 8 s. These were then incubated with 200 μL of glutathione beads as described above, centrifuged carefully at 1000g for 1 min, then washed 3 times with bacterial lysis buffer and once with cold PBS and stored at 4 °C for a maximum period of 1 week.

In the meantime, 300 mL liquid culture of *D. discoideum* AX3 cells in HL5 medium was grown in room temperature until cell density of 8.5×10^6/mL. They were centrifuged as described previously, resuspended in 20 mL of TNE buffer with 0.1% Tx-100 and centrifuged at 75,000 g for 30 min. A protein concentration of the resulting sample was approx. 5 mg/mL as determined with Precision Red (Cytoskeleton, USA).

After an aliquot of each bound GST-fusion protein was analyzed on SDS PAGE, 10 μg of each protein was mixed with 10 mL of AX3 lysate and incubated for 2 hours at 4 °C. After the incubations, beads were centrifuged down (1,000g, 1 min), washed 4 times consecutively with TNE and boiled in NuPAGE sample buffer for 10 min at 100 °C. SDS PAGE gel was then analysed at the mass spectrometry unit, as described above.

For pulldown from mammalian cell lysate, approximately 1.5×10^7 U2OS cells were harvested as described above. The rest of the protocol remained the same as in *D. discoideum* experiments.

4. Results

4. 1. Overexpression and endogenous protein detection of FAM21 in U2OS cell line

U2OS human cell line was transiently transfected with either FAM21-eGFP or FAM21-myc, fixed, and, in the case of myc-tagged FAM21, immunostained with anti-myc antibody for immunofluorescence (**Figure 6A, B**). After 24 hours, most transfected cells detach from the surface and die; however, control transfections using different constructs were not toxic to cells (data not shown). The toxicity of FAM21-myc was somewhat lower than that of GFP-tagged FAM21. Myc-tagged fusion protein was therefore used in most subsequent experiments requiring transfection. Still, a stable cell line could not be generated because the FAM21-overexpressing cells ceased to divide, developed extensive thin projections (**Figure S1**) and eventually all died during the course of several weeks.

Figure 6 – Overexpression and endogenous protein detection of FAM21 in U20S cell line. (**A**) FAM21-eGFP-expressing cell; (**B**) FAM21-myc-his-expressing cell; (**C**) Verification of the FAM21-myc-his signal using anti-FAM21 antibody – the signals colocalize except for a nuclear signal of anti-FAM21 antibody which is very weak in (**D)** a strongly overexpressing cell and thus probably represents non-specific binding. Scale bar: 10 μm.

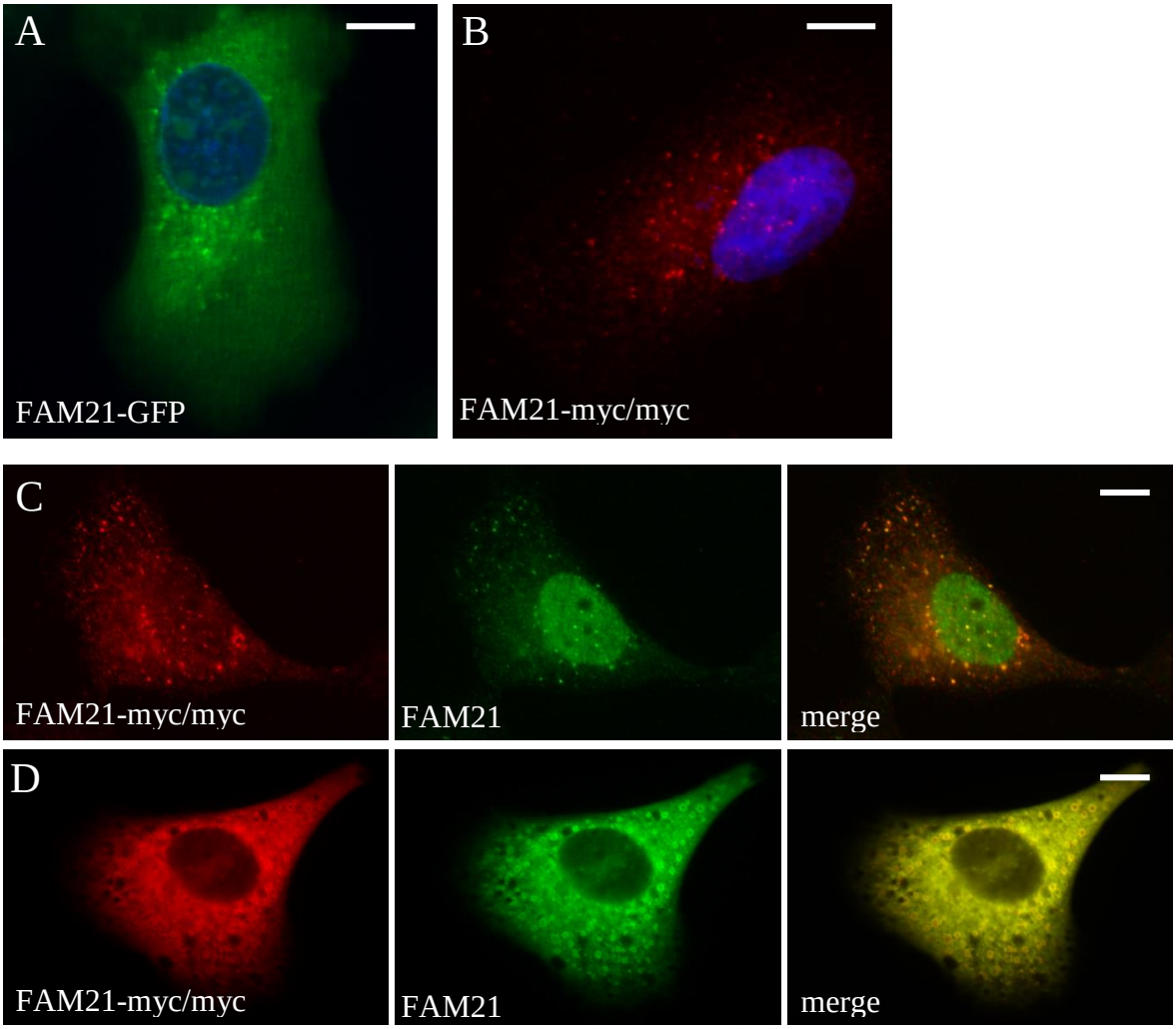

Trustworthiness of the FAM21-myc overexpression phenotype was corroborated using a commercial antibody against FAM21 (**Figure 6C**). Anti-myc antibody signal colocalizes with the anti-FAM21 antibody signal. The antibody against endogenous FAM21 produces a strong signal in the nucleus regardless of the transfection. The anti-myc antibody does not produce this signal and strongly overexpressing cells have the same amount of FAM21 signal in the nucleus as weakly overexpressing cells (**Figure 6D**); this suggests that the nuclear signal of anti-FAM21 antibody is non-specific. Same conclusion is supported by the fact that wild-type

cells have the same intensity of anti-FAM21 antibody signal in their nucleus as those transfected with FAM21-myc (data not shown).

Expression of FAM21-myc in transiently transfected cells was verified by SDS PAGE/Western blot (**Figure 7**).

Figure 7 – FAM21-myc is expressed in U2OS cells transiently transfected with the corresponding construct.

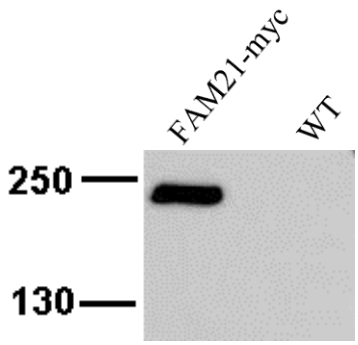

WB: α-myc

4. 2. Localization of FAM21 to the early endosomes

Fluorescence microscopy was used to investigate subcellular localization of protein FAM21. All data was acquired on fixed cells using various combinations of anti-myc and anti-FAM21 antibody with markers of the early endosomal compartment. All acquired data for overexpressed FAM21-myc are consistent with those for endogenous FAM21 investigated using anti-FAM21 antibody.

Figure 8 – Localization studies of FAM21 at the early endosome. (**A**) FAM21 colocalizes with overexpressed mouse WASH-GFP. (**B**) FAM21-myc localizes to EEA1-coated vesicles representing early endosomes. (**C**) FAM21 localizes to early and sorting endosomes positive for Alexa 594-conjugated transferrin (**D**) FAM21 localizes to Hrs-decorated vesicles, primarily early endosomes. Scale bar: 10 μm.

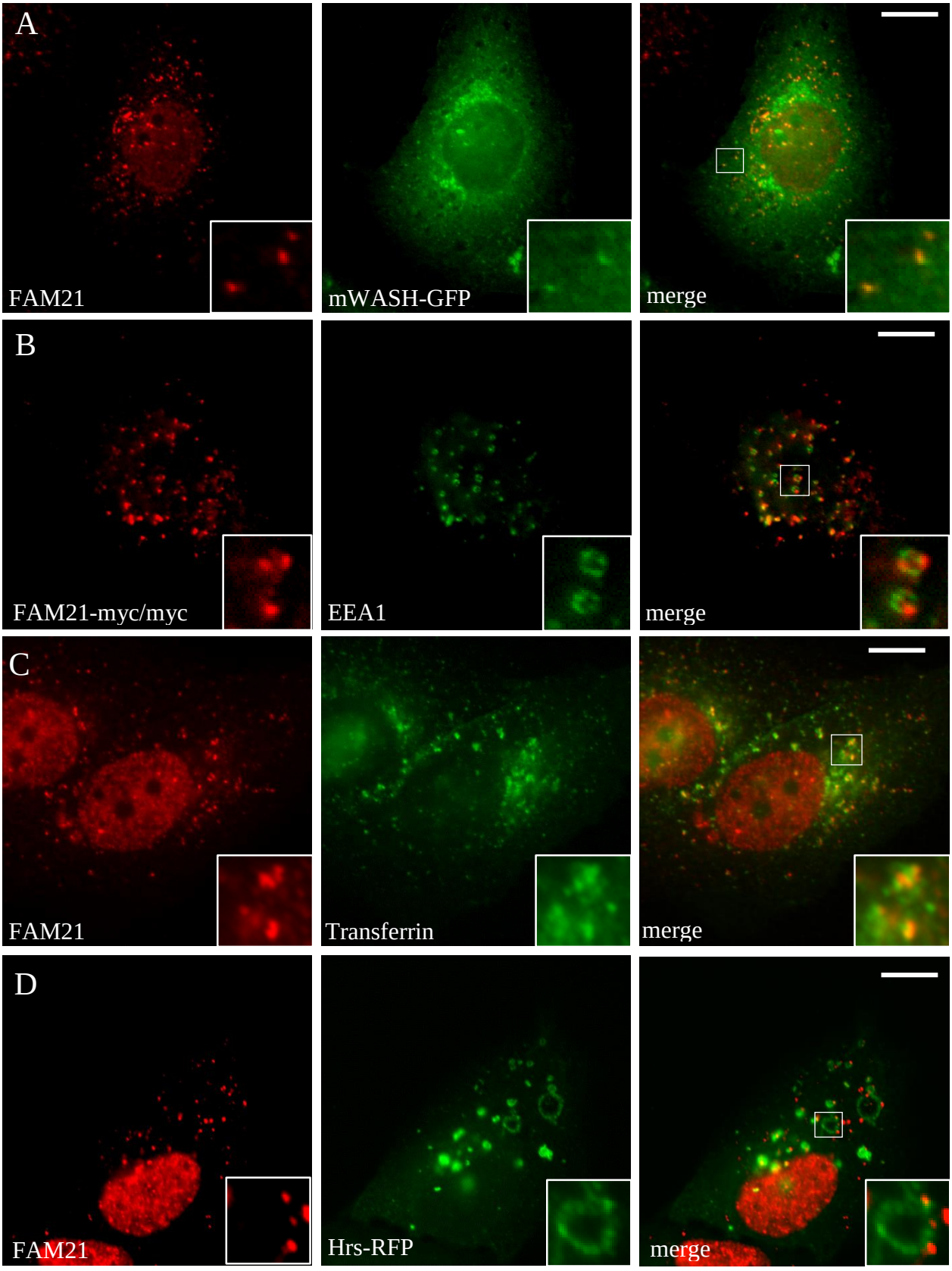
A
FAM21
mWASH-GFP
merge
B
FAM21-myc/myc
EEA1
merge
C
FAM21
Transferrin
merge
D
FAM21
Hrs-RFP
merge

The experiments were preceded by evaluating if FAM21 colocalizes with other WASH complex components. This was achieved via transient transfection of the pEGFP-mWASH vector expressing a mouse homologue of the WASH gene (**Figure 8A**). As in the case of other GFP-tagged subunits of the WASH complex, mouse WASH is expressed very strongly and is found in the entire cytoplasm. However, it is enriched at FAM21-positive vesicles and the majority of the endogenous FAM21 colocalizes with WASH-GFP puncta although some WASH puncta remain FAM21-negative. Colocalization pattern of two simultaneously detected subunits at endogenous expression levels was not analysed but an even higher colocalization would be expected in such experimental setting.

FAM21-myc clearly localizes to vesicles that stain with antibody against early endosomal antigen 1 [EEA1] (**Figure 8B**), a hallmark of early endosomes (Mu et al., 1995). Similar localization pattern of FAM21-myc is seen with antibody against Rab5 (data not shown), another established marker of early endosomes (Simonsen et al., 1998). FAM21 also colocalizes with Alexa 594-conjugated transferrin after 120 min of chase during which transferrin is internalized and transported through early and sorting endosomes (**Figure 8C**). Next, localization of endogenous FAM21 in Hrs-RFP transiently expressing cells was evaluated. Overexpression of Hrs, a prototypical early endosomal protein (Bache et al., 2003), causes a dramatic increase in the size of endosomes and association of FAM21 with these structures provides a strong evidence for the occurrence of FAM21 at the early endosomes (**Figure 8D**).

Interestingly, FAM21 signal never actually overlaps with that of early endosomal markers. The highest, yet still partial overlap is seen between FAM21 and transferrin. Hrs, Rab5 and EEA1 spatially associate with FAM21 puncta but FAM21 always localizes to distinct spots (see insets in **Figure 8B** and **8D**). To confirm the spatial separation between FAM21-myc and EEA1, samples were analyzed using structured illumination super-resolution microscopy (SIM). The super-resolution image (**Figure 9B**) provides additional detail (compare with **Figure 9A**, which represents a computer-created wide-field image). Various insets of the image (**Figure 9C**) confirm the spatial separation of EEA1 and FAM21 into distinct membrane microdomains.

FAM21 also does not overlap with F-actin - FAM21 rather forms puncta around the actual F-actin patches visualised with fluorophore-conjugated phalloidin on high-resolution images acquired with structured illumination microscopy (**Figure S2A**). FAM21 puncta also do not

colocalize with DiI-stained endosomal membranes (**Figure S2B**). The actin patches themselves colocalize well with the endosomal membrane (**Figure S2C**).

Figure 9 – Super-resolution imaging of FAM21 at early endosomes using structured illumination microscope (SIM). (**A**) Pseudo-widefield image generated from the super-resolution data (**B**) Super-resolution reconstructed image generated from the same data. Scale bar: 10 μm. (**C**) Various insets of picture 9B showing spatial separation of EEA1 and FAM21 microdomains. Scale bar: 1 μm.

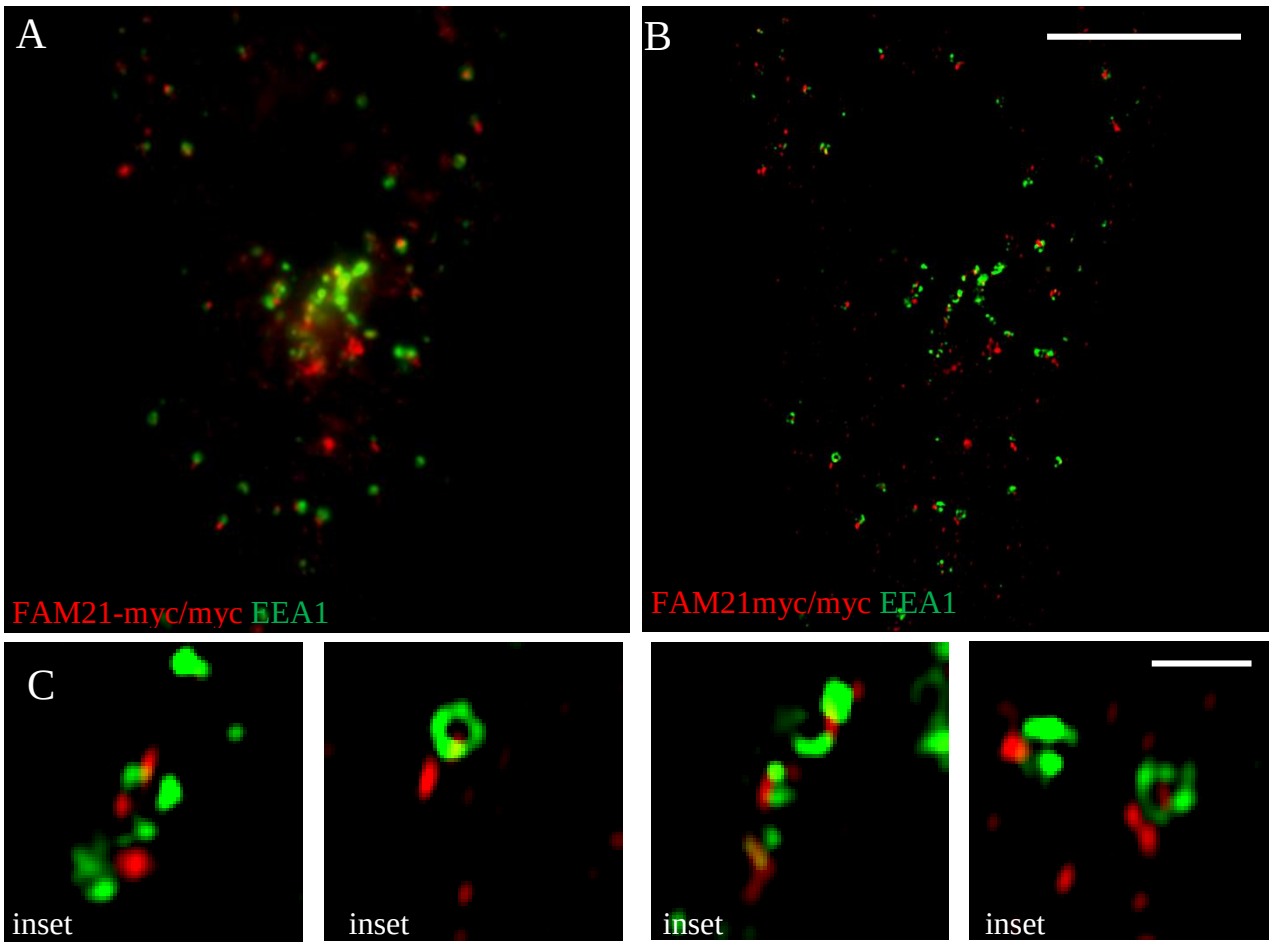

4. 3. FAM21 in non-early endosomal compartments

After the localization of FAM21 to the early endosomes was confirmed, similar analysis was conducted on other endomembrane compartments of the U2OS cells where FAM21 is suspected to localize. First, a Rab11-GFP stable cell line was transfected with FAM21-myc. Rab11-GFP localizes to two distinct compartments, which are very well pronounced in the

Rab11-GFP stable cell line (**Figure 10A**). A subset of Rab11 is found at the early endosomes, together with EEA1 and FAM21. Additionally, Rab11 also forms EEA1-negative FAM21-positive large perinuclear compartments which are likely to represent recycling endosomes.

Figure 10 – FAM21 in other endosomal compartments. (**A**) FAM21-myc-his localizes to Rab11-positive compartment in a Rab11-GFP-transfected cell line. Arrow points to a FAM21-positive Rab11 vesicle that contains EEA1; star labels a larger perinuclear endosomal structure positive for FAM21 and Rab11 but negative for EEA1. (**B**) FAM21-myc-his decorates Rab7-positive structures, mostly late endosomes. (**C**) FAM21-myc-his associates with LAMP1-positive endosomes (lysosomes). (**D**) Endogenous FAM21 does not colocalize with the Golgi apparatus. (**E**) Quantification of EEA1-, Rab7- and LAMP1-associated FAM21 puncta. Maximum projections from Z-stacks; scale bar: 10 μm.

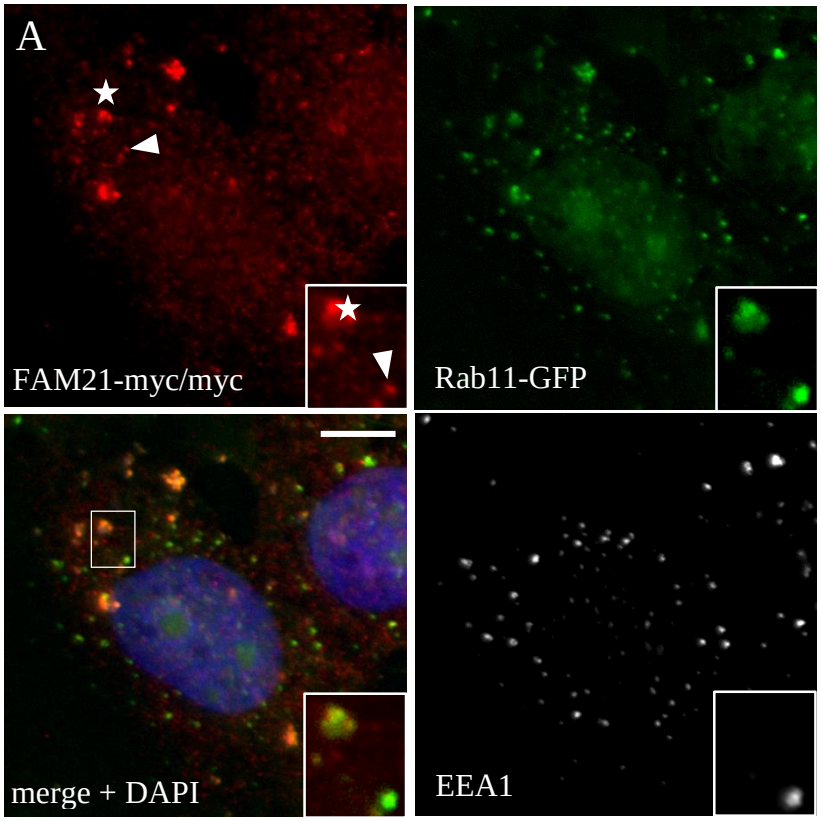

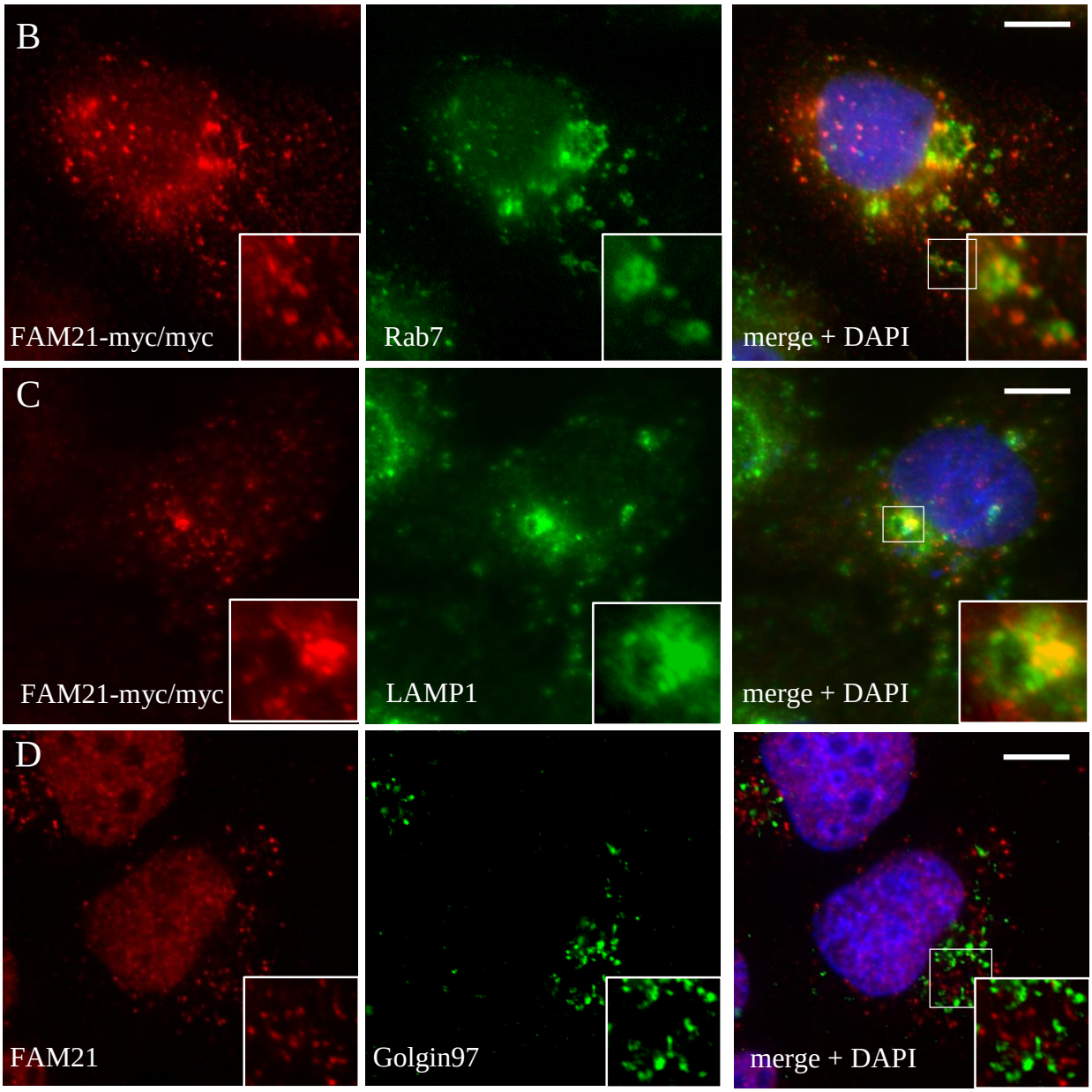
B
FAM21-myc/myc
Rab7
merge + DAPI
C
FAM21-myc/myc
LAMP1
merge + DAPI
D
FAM21
Golgin97
merge + DAPI

E

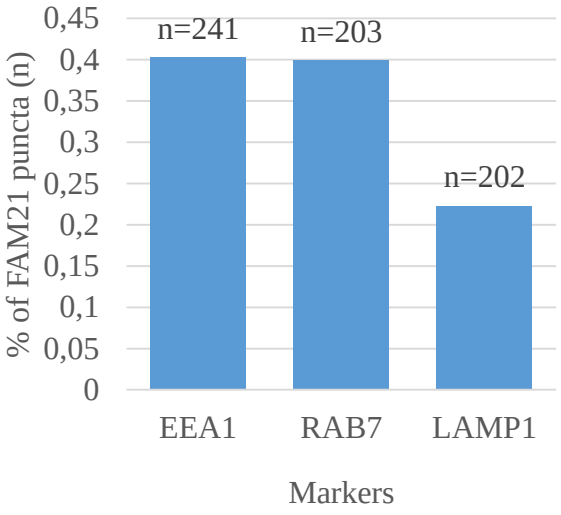
0,45
0,4
0,35
0,3
0,25
0,2
0,15
0,1
0,05
0
% of FAM21 puncta (n)
n=241
n=203
n=202
EEA1
RAB7
LAMP1
Markers

Localization of FAM21 to the downstream compartments of the degradation pathway was then evaluated. FAM21-myc forms puncta on the membrane of late endosomes (which were identified as Rab7-positive and mostly perinuclear endosomes; **Figure 10B**). Membrane microdomains with FAM21 are observed on a majority of late endosomal structures. A weaker yet clearly present association is seen between FAM21 and LAMP1 [lysosomal-associated membrane protein 1]; a subset of lysosomes associates with FAM21 (**Figure 10C**). On the contrary, FAM21 does not colocalize with Golgin97, a marker of the Golgi apparatus (**Figure 10D**). In this case, endogenous FAM21 was monitored instead of FAM21-myc because the simultaneous staining with anti-myc and anti-Golgin97 would not be possible using available antibodies. FAM21 thus associates with a variety of endomembrane compartments but not the Golgi apparatus.

The percentage of EEA1-associated, Rab7-associated and LAMP1-associated FAM21 puncta was then quantified. FAM21 puncta were described as EEA1/Rab7/LAMP1-associated when the corresponding regions of interest (ROIs) were located less than 0.25 μm laterally from vesicular structures stained with these endosomal markers. 40.2% of FAM21 puncta associate with EEA1, 39.9% associate with Rab7 and 22.2% associate with LAMP1 (**Figure 10E**).

4. 4. New interaction partners of FAM21 in *D. discoideum*

The preceding results showed that FAM21 is found in a variety of cellular compartments, in each surrounded by a characteristic meshwork of membrane-associated actin and other proteins. We hypothesized that the currently known interaction partners cannot fully explain the occurence of FAM21 in these cellular locations.

A protein-protein interaction assay was then conducted to expand the list of known FAM21 interaction partners. FAM21 is a difficult protein for biochemical analysis because adequate amounts of the protein are difficult to isolate from mammalian cells, where FAM21 is toxic and attempts to create a stable cell line failed. Therefore, a slime mold *Dictyostelium discoideum* was used as a model for this part of the project. A cell line expressing GFP-FAM21 in a FAM21 knock-out background had already been generated (Park et al., 2013). Despite the evolutionary distance between humans and *Dictyostelium,* parts of the sequence are conserved throughout their full length (**Figure 11A**). First, cell lines expressing the GFP-tagged protein of interest (FAM21) and a control (MROH1) were verified using fluorescence microscopy (**Figure 11B**) and Western blot approach (**Figure 11C**).

Figure 11 – *Dictyostelium discoideum* as a model to study FAM21 interaction partners. (**A**) Similarity plot of amino acid sequences of human FAM21C protein (UniProt code Q9Y4E1) and *Dictyostelium discoideum* FAM21 (UniProt code Q552E2). Created in NTI Vector – height of bars represents a running average of sequence similarity, x-axis in arbitrary units. (**B**) Subcellular localization of GFP-FAM21 and MROH1-GFP in *Dictyostelium discoideum*; single scan on confocal microscope. Scale bar: 10 μm. (**C**) Western blot of these cell lines with proteins of interest visualized using anti-GFP antibody.

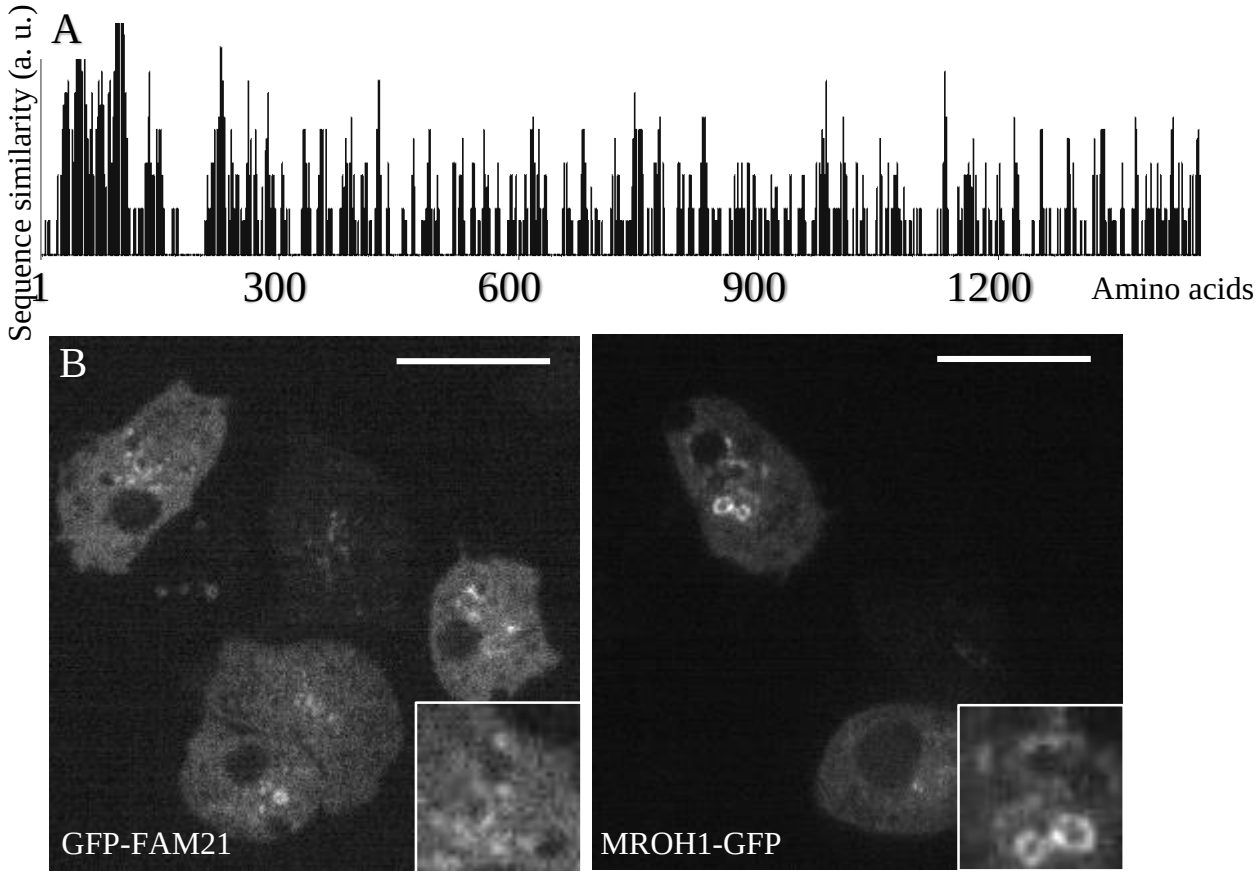

A whole-cell crosslinking-based analysis of interaction partners was employed; during the procedure, proteins in association with each other are covalently crosslinked together. Fundamentally, the crosslinking step happens simultaneously with cell lysis, which ensures that protein interactions in their physiological conditions are captured. This was followed by high-affinity GFP-trap purification and mass spectrometry protein identification (see experimental procedures for a detailed description).

Importantly, half of each sample was analysed in the crosslinked state while the second half was decrosslinked by heat. Proteins of small molecular weight are better seen in crosslinked samples while proteins of high molecular weight are better analysed in the decrosslinked state. This is important because the total unique peptide count (TUPC) is used as a semi-quantitative measure of protein abundance in the sample (Kumar and Mann, 2009). A small part of each sample volume was analysed on a separate SDS PAGE/Western blot and stained with anti-GFP antibody to show the effect of crosslinking and heat decrosslinking (**Figure 12**).

Figure 12 – Analysis of FAM21 interacting proteins using a crosslinking-based GFP-Trap purification approach. Western blot of a small aliquot of samples that were sent for mass spectrometry analysis. The image shows bands of original protein and a smear of crosslinked (CL) proteins above them. The smear is partially reversed by heat decrosslinking (deCL) of formaldehyde bonds.

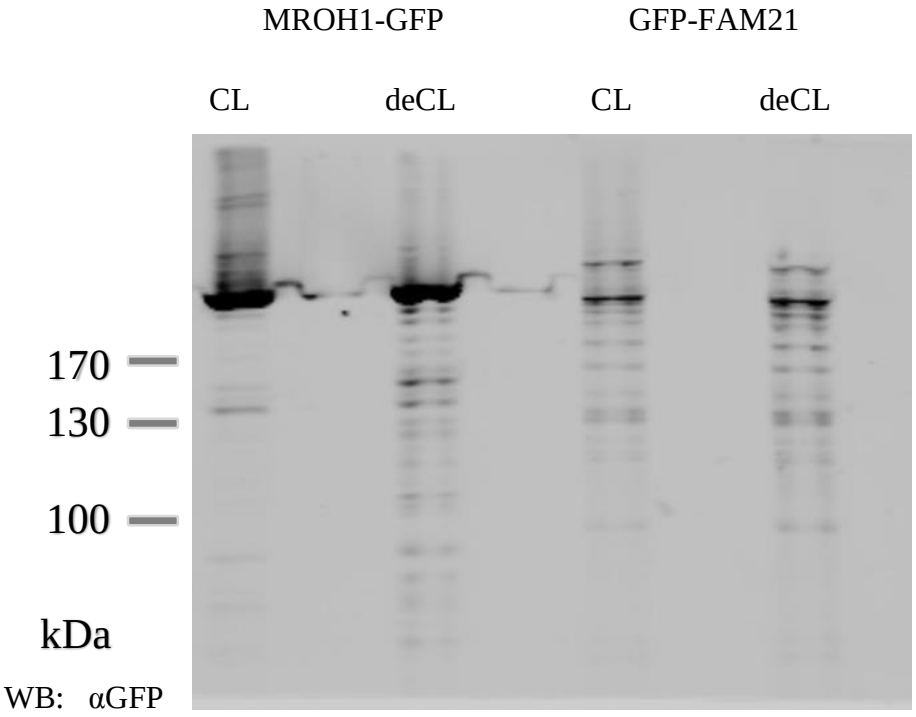

GFP-FAM21 crosslinked and decrosslinked sample yielded 1601 and 1736 proteins, respectively. A convenient method to differentiate real interacting partners from the cellular background must thus be employed. *D. discoideum* cell line expressing MROH1-GFP, a protein which localizes to the same vesicles as FAM21 but does not constitute a part of the WASH complex (unpublished data), was used. MROH1-GFP cell line was analysed in parallel to GFP-FAM21 in an identical manner, yielding 962 and 1564 proteins in the crosslinked and uncrosslinked sample, respectively. The data file of interacting proteins was then manually scanned for proteins which appear enriched in the FAM21 samples compared to the MROH1 sample; molecular size of the proteins was considered when discrepancies arose between the crosslinked and the uncrosslinked samples. Such approach helps to discriminate between specific protein-protein associations – which are the desirable outputs of our assay – and general localization of abundant proteins (such as actin) to the vesicular surface.

Selected "hits" are summarized in **Table S1**. Several already known interaction partners of FAM21 – mostly described from human cell lines - are also associated with FAM21 in *D. discoideum*. SWIP, strumpellin, WASH and CCDC53 were among the best hits, FAM21 is thus strongly associated with all the other published components of the classical WASH complex; the association is strongest with SWIP and strumpellin. Comparatively weaker, yet still very strong association was detected for WASH and CCDC53.

The screen also demonstrates enrichment of coiled-coil proteins CCDC22 and CCDC93, two subunits of the recently described, yet enigmatic CCC complex. Its other components, UPF0505 and COMMD proteins were also detected in various amounts. Many components of the ubiquitin machinery were also found in the assay. Cullin-3 and COP9 (Constitutive photomorphogenesis 9) signalosome subunits (CSN5, CSN7) represent the strongest hits. Many other ubiquitination components are also present in the sample but are not significantly enriched compared to the control sample, suggesting that these are not as specific to the WASH complex as those listed above. Two candidates for a functional component of the ubiquitination machinery – ubiquitin ligases – were pinpointed: TRAF6 [Tumor necrosis factor-receptor associated factor 6]-like protein DDB_G0273433 and a TRIM3 [tripartite motif 3]-like protein DDB_0185353. The latter is extremely enriched and represents a strong new candidate for a WASH complex interaction partner.

Several actin-associated proteins were also enriched in FAM21-crosslinked sample compared to the MROH1 sample. Examples of such actin-associated proteins include CARMIL (Capping

protein, Arp2/3 and myosin I linker), myosin-I and IB heavy chains, comitin, fimbrin, villin headpiece-domain containing protein, gelsolin-related protein and also focal adhesion proteins vinculin and talin-B. Additionally, Rab proteins Rab7A and Rab14 were found.

Some proteins enriched in FAM21 remain poorly explicable by the theoretical background that science has on FAM21. For example, there is a significant enrichment of several nucleolar proteins such as RNA-binding protein 28 (RBM28) and ribosome production factor 2 homolog (RPF2). Remarkably, several discoidin domain-containing proteins were also highly enriched – galactose-binding domain-containing protein (DD7-1), discoidin-1 subunits A, B/C and D as well as discoidin-2. Other unclassifiable hits include FAM45 and serine/threonine protein phosphatase PP1.

On the other hand, some proteins previously shown to interact or associate with FAM21 or the WASH complex were not detected. These include retromer components Vps35, Vps29 and Vps26, but also capping proteins, sorting nexins, FKBP15 and subunits of the BLOC complex.

4. 5. Binding partners of the LFa motifs of FAM21

The interaction assays were followed by investigations to determine which proteins bind to various portions of the FAM21 C-terminal tail because this domain is currently suspected to harbour most of the binding sites for interaction proteins (most prominently, at the LFa motifs). Four fragments were amplified from the FAM21 *D. discoideum* gene: "TAIL1" (the complete C-terminal tail, positions 943-4440), "TAIL2" (lacking a conserved C-terminal region with unknown function, positions 943-4128), "TAIL3" (lacking a portion of gene that includes the capping protein-binding region, positions 943-3600) and "TAIL4" (representing 7 most N-terminal LFa motifs present in the gene, positions 943-1668).

The amplified regions are shown in **Figure 13A** and the corresponding PCR products are in **Figure 13B**. Fragments were then fused with GST, sequence-verified, expressed in BL21 bacteria and purified using glutathione beads. The resulting products were analysed by SDS PAGE (**Figure 13C**). TAIL1 and TAIL2 are both very unstable (comparable results were obtained when bacteria were grown for 6 hours at 30 °C or overnight at 22 °C). TAIL3 is not produced at all and only its GST tag is expressed. Adequate amounts of TAIL4 are present and only TAIL4 was used in subsequent experiments.

10 μg of GST-TAIL4 were incubated with *D. discoideum* lysate. Same amounts of GST were used as a control experiment. Complete pulldowns from these incubations were analysed on

LC-MS/MS. 31 proteins were detected in the GST-TAIL4 sample, six of which were disqualified as contaminants because they were present in the GST control and one was FAM21 which was present in the sample as the bait. Specific hits encountered in this assay are summarized in **Table 3**.

Figure 13 – Analysis of protein-protein interactions of FAM21 C-terminal tail fragments. (**A**) Four fragments amplified from the *D. discoideum* FAM21 gene are shown. (**B**) Corresponding PCR fragments amplified from the FAM21 gene. (**C**) SDS PAGE of GST-fused fragments expressed in BL21 bacteria and purified using glutathione beads; gel is stained with InstantBlue. Only FAM21 TAIL4 is expressing in adequate amounts.

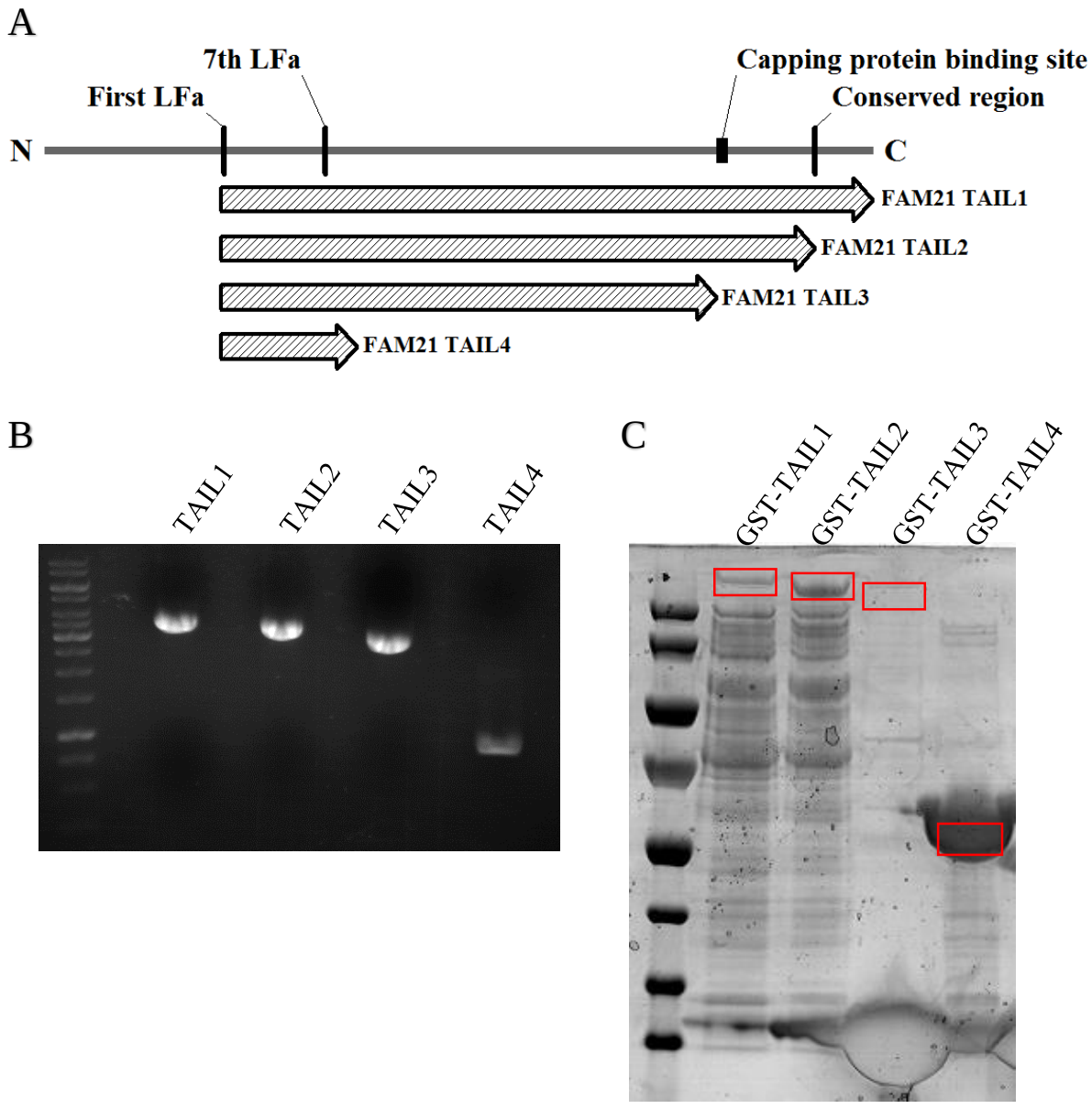

Table 3: Interaction partners of LFa motifs detected in the GST-pulldown using GST-TAIL4 fragment incubated with *D. discoideum* lysate. TUPC shown as a proxy for the quantity of proteins in the sample.

Protein name	**TUPC (control)**	**TUPC (sample)**
CCDC22	0	3
CCDC93	0	3
AP-2 α2	0	4
PP1	0	4
FAM45	0	4
FKBP4	0	2
CmfB	0	2

D. discoideum GST-TAIL4 protein was then "ectopically" incubated with mammalian lysate prepared from U2OS cells, using identical experimental procedure. However, instead of separating the sample on SDS PAGE, sample on glutathione beads was only resuspended in 100 μL triethylammonium bicarbonate buffer (TAEB, Sigma-Aldrich, USA) and boiled at 97 °C for 10 min. Pulldown with unfused GST was used as a control sample. 204 proteins were detected in the GST-TAIL4 sample, 105 of which were disqualified because they were not at least 4 times enriched compared to the control. Strongest hits are summarized in **Table 4**.

Table 4: Interaction partners of LFa motifs detected in the GST-pulldown using TAIL4-GST fragment incubated with U2OS cell line lysate. Scores provide a measure for the quality of the hit in the corresponding sample.

Protein name	**Score (control)**	**Score (sample)**
PP1 catalytic subunit α	26	3 457 500
PP1 catalytic subunit β	0	18 559 000
PP1 catalytic subunit γ	0	8 274 800
Vps35	0	893 625
Myosin IIb heavy chain 4 (MYH4)	0	119 190 000
RING finger protein 44 (RFP44)	0	34 930 000
Liprin-β1	0	13 068 000
SNX27	0	551 690

A more sensitive annotation of the results (using Swissprot) uncovered additional hits including Rab10, Rab14, cell division control protein 42 (Cdc42), cullin-1 and vacuolar protein-sorting associated protein 26B (Vps26B).

4. 6. Experiments on Vps35 – FAM21 association in U2OS

The preceding results created a need to re-evaluate the importance of retromer component Vps35 for the localization of FAM21 to endosomes in mammalian cells. U2OS cells were transfected with Vps35 siRNA (5'-CCACGUUGAUCAGAUCA-3', Silencer Select Predesigned, Ambion, USA) and the efficiency of the siRNA-mediated silencing was confirmed using quantitative PCR. 48 hours after the knock-down, Vps35 mRNA levels were down to 16 % of the levels in wild-type cells (**Figure 14A**).

The effects of Vps35 knock-down on localization of transfected FAM21-myc in respect to EEA1, Rab7 and LAMP1 were then evaluated. There is no clear change in the phenotype visible to the naked eye (images not shown). FAM21 remains localized to the same intracellular compartments and there is no apparent shift in the levels or localization pattern of FAM21 puncta (**Figure S3**). These observations were then quantified. Pearson coefficient, the method of choice for most colocalization experiments, is not suitable - it does not reflect the fact that FAM21 often resides on endosomes but does not actually colocalize with EEA1 or other endosomal markers (it localizes to distinct membrane microdomains). Additionally, it is time-consuming and quite sensitive to individual levels of FAM21-myc in each cell.

The qualitative results were thus quantified using a different computational method. Cells were again transfected with FAM21-myc and labelled for either EEA1, Rab7 or LAMP1. FAM21 puncta were automatically annotated and a 0.25 μm-wide band was added to them. Signal intensity in these "extended" FAM21 puncta ("puncta intensity") was then compared to an average intensity of the image ("image intensity"). Finally, puncta/image intensity ratios were plotted for the control and the Vps35-silenced sample (**Figure 14B**). The data can be better visualised on a histogram-like frequency chart (**Figure 14C**) where puncta/image intensity ratios are calculated for each vesicle (x-axis) and plotted by frequency (y-axis). Higher puncta/image intensity ratio implies stronger association of the FAM21 puncta with endosomal markers. Results indicate that all three endosomal markers are mildly affected by Vps35 knock-down but the difference is not statistically significant because of enormous variability present in the data for individual vesicles.

Figure 14 – FAM21 localization and role of the retromer. (**A**) Efficiency of the Vps35 siRNA-mediated silencing evaluated using real-time PCR. (**B**) Quantification of EEA1, Rab7 and LAMP1 signal in the 0.25 μm vicinity of FAM21 puncta in wild-type and Vps35-silenced U20S. n = number of FAM21 puncta analysed. Error bars - standard deviation. Puncta/image intensity ratio normalized to the wild-type. (**C**) Frequency chart of puncta/image intensity ratios from (B); higher intensity ratio suggests higher occurrence of marker signal in the vicinity of FAM21 puncta.

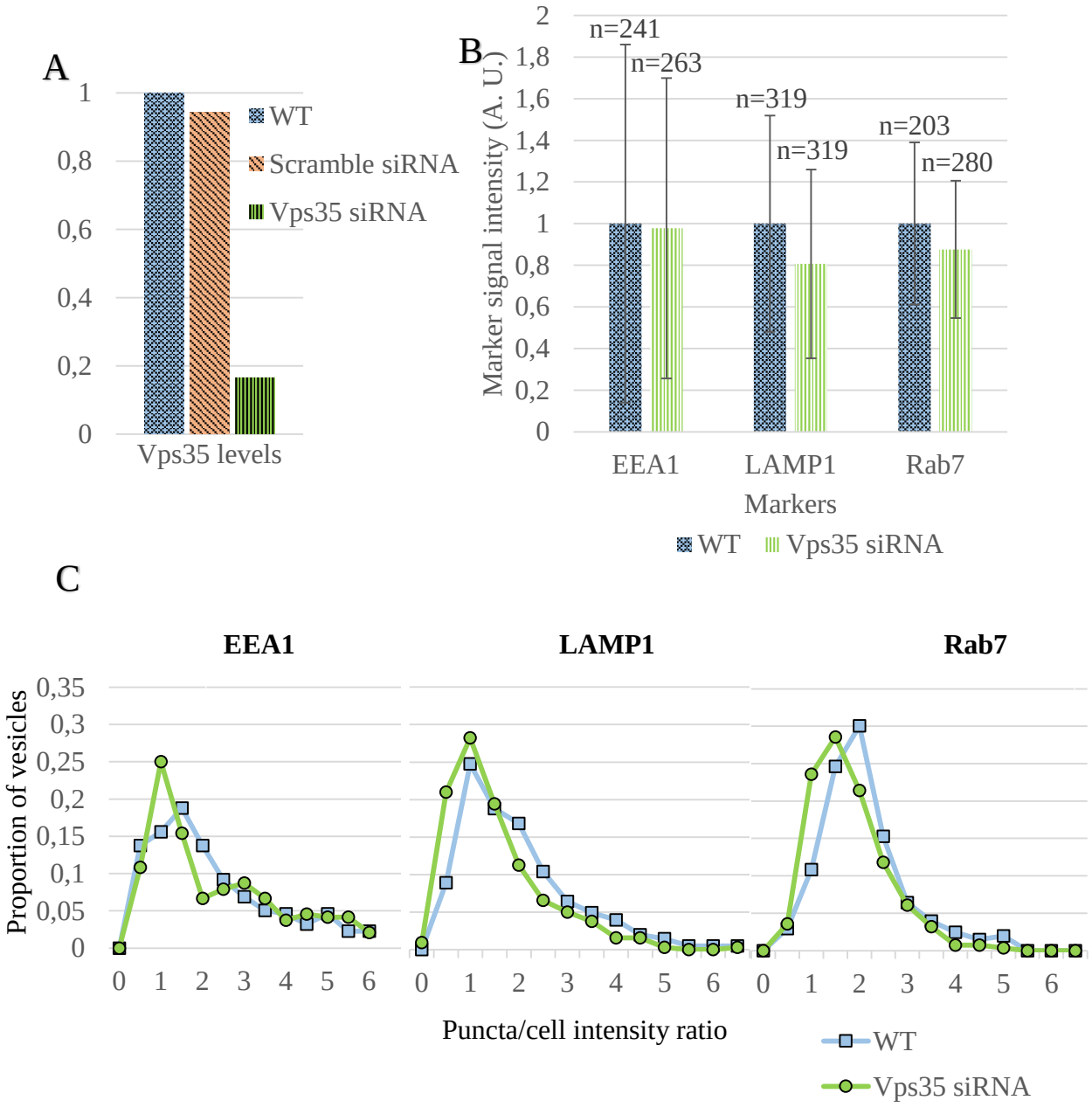

5. Discussion

A key aspect of this thesis is the usage of two model organisms, each of them offering different approaches. Human cell lines are very practical for microscopy due to the cell size, knowledge of the intracellular trafficking routes and availability of antibodies. *D. discoideum*, with its short cell cycle and easy genetic manipulation, is more suitable for large-scale biochemical studies. Combination of both model organisms allows us to extract the conserved principles which govern cell physiology and separate them from derived properties specific to one branch of the eukaryotic tree of life. This is especially relevant to the life style of both species – while *D. discoideum* relies heavily on feeding via phagocytosis, vesicular trafficking in mammalian cell lines is more concerned with recycling and signalling (Insall, 2013).

Separated by 1.5 billion years of independent evolution, the relevance of *D. discoideum* research on FAM21 to our understanding of mammalian cell has been questioned (Seaman et al., 2013). However, certain N-terminal portions of the FAM21 protein are approx. 60% conserved between human and the slime mold. While the C-terminal portion is much less conserved, the LFa motifs are clearly present in *D. discoideum* (Insall, 2013) and can arguably bind the same interaction partners.

5. 1. FAM21 localization

The first goal of my diploma thesis was to assess subcellular localization of FAM21 in mammalian cells. I used microscopic approaches to define the specific vesicular subpopulation with which FAM21 is associated in human osteosarcoma cell line U2OS. Two approaches were generally feasible: 1) expressing a tagged version of FAM21 and 2) detecting the endogenous FAM21 protein. In this thesis, both experimental methods were combined and cross-validated against each other, whenever possible. Overexpression of tagged FAM21 enabled me to use good-quality anti-myc antibodies and combine them with antibodies against several markers of endosomal compartments.

However, most transfected cells detach from the surface and die within 24-48 hours post-transfection, supporting previous reports that overexpression of FAM21 is toxic to cells (Harbour et al., 2012). This precluded the isolation of tagged FAM21 for analysis of interaction partners. Because transfection of different constructs was not detrimental to cell growth, the massive cell death is probably caused by the overexpression of protein FAM21 inside the transfected cells. Anti-FAM21 antibody enables to study the endogenous levels of FAM21 in cells and thus offers a less artificial overview of FAM21 in cells. However, its use in

biochemical studies would be also impossible as it suffers from a high levels of non-specific binding, especially in the nucleus. Specific signal in the nucleus was not observed and the recently published reports of nuclear FAM21 (Deng et al., 2014; Verboon et al., 2015) thus were not confirmed.

Using a combination of both approaches, I confirmed localization of FAM21 to EEA1-positive endosomes, representing early endosomes (Mu et al., 1995). Same results were obtained using Rab5 as a marker – rather unsurprisingly because EEA1 is an effector protein of Rab5 (Simonsen et al., 1998) – as well as Hrs, an early endosomal protein which recruits so-called ESCRT (endosomal sorting complex required for transport) complex to endosomes (Bache et al., 2003; Komada and Kitamura, 1995). Usage of Hrs was advantageous because it increased the size of early endosomes, improving the visibility of endosomal membrane microdomains of FAM21. Using all these markers, I localized of FAM21 to specific membrane microdomains of early endosomes in a similar way as reported in early publications (Gomez and Billadeau, 2009) and for the first time visualized these microdomains using super-resolution microscopy.

Localization of FAM21 to other vesicular compartments – late endosomes and lysosomes – has also been addressed in this thesis. The prevailing scientific opinion has been that the localization to these compartments is less frequent and happens on a rather small scale (Derivery et al., 2009; Seaman et al., 2013). On the contrary, I found that FAM21 puncta localize to Rab7-positive late endosomes to the same amount as they do to EEA1-positive early endosomes – and about twice more than to lysosomes. In absolute numbers, about 40% of FAM21 puncta are associated with the marker of early endosomes, 40% are associated with a marker of late endosome and about 20% are associated with a marker of lysosomes. The underestimation of the late endosomal and lysosomal FAM21 in past studies has several possible explanations. First, different cell lines were used, where the distribution of FAM21 can vary. Secondly, it is more demanding to estimate localization of FAM21 to an endolysosomal compartment because late endosomes and lysosomes are more fluid than early endosomes and their signal is more dispersed.

However, the theoretical sum of these percentages (~100%) does not mean that FAM21 puncta only localize to early or late endosomes or lysosomes. The spatiotemporal separation of the endosomal markers is not absolute. Actually, a majority of endolysosomal vesicles in the cell are both Rab7- and LAMP1-positive (Szymanski et al., 2011). As Rab7 and LAMP1 usually localize to distinct membrane subdomains of these “endolysosomes” (Szymanski et al., 2011),

I speculate that FAM21 localizes to Rab7-coated parts more than it does to LAMP1-coated portions. Additionally, it is very plausible that FAM21 localizes to other distinct subcompartments (e.g. autophagosomes, various types of recycling vesicles) but they are either rare in U2OS cells or associate with markers used in my experimental setting (such as I have shown for the recycling endosome marker Rab11).

This thesis did not attempt to similarly evaluate the subcellular localization of FAM21 in *D. discoideum*. The deciphering of the elementary principles of vesicular trafficking pathway in *D. discoideum* is still underway even though some progress has been made (Maniak, 2011; Neuhaus et al., 2002); the use of precise markers of endosomal compartments is not well established in *D. discoideum*. However, functional studies from *D. discoideum* suggest that the WASH complex has important roles in the lysosomal system (King et al., 2013; Park et al., 2013).

5. 2. FAM21 interaction partners

Occurrence of FAM21 on late endosomes and especially lysosomes is in stark contrast to the localization of retromer subunit Vps35, a major binding partner of FAM21 (Helfer et al., 2013; Jia et al., 2012). Retromer does not have a defined role in the endolysosomal compartment (Seaman et al., 2013) and Vps35 component of the retromer does not colocalize with LAMP1-positive lysosomal structures (McGough et al., 2014a). This has led me to inspect the currently known interaction partners of FAM21 and explore the potentially new.

Protein interaction assays notoriously suffer from a high percentage of false positives and negatives. For example, some authors can only detect the interaction between FAM21 and Vps35 in low-stringency HEPES-based buffers (Zavodszky et al., 2014). Therefore I analysed protein-protein interactions using a crosslinking assay which allows easy interpretation of experimental data: all proteins found in the vicinity of GFP-FAM21 are covalently crosslinked to it and their enrichment can be measured against a strong control MROH1 – a protein found on the same vesicles but not physically interacting with the WASH complex. One disadvantage of a strong control is that some interaction proteins which are common to both the protein of interest and the control are lost. Another weakness of the crosslinking approach is that not all enriched proteins represent direct interaction partners – the enrichment can be caused by mere presence of high amounts of proteins in the vicinity of GFP-FAM21 or by interaction through a mediator which binds both proteins. On the positive side, the crosslinking assay is able to detect even weak associations. Additionally, the use of *D. discoideum* is advantageous because

GFP-FAM21 re-expression in a FAM21-knockout background enables close-to-natural levels of the fusion protein in cells.

Detection of previously published FAM21 interaction partners suggests that the crosslinking approach is viable. All WASH components were found to be enriched but strumpellin and SWIP produced an especially strong signal. This could mean that the FAM21, strumpellin and SWIP together form an extremely specific subcomplex, although data from human cell lines indicate that only SWIP and WASH are direct binding partners of FAM21 in the WASH complex (Harbour et al., 2012). Interestingly, the screen also supports association with interaction partners of FAM21 that have been published recently – CCDC93, CCDC22 and COMMD proteins (Phillips-Krawczak et al., 2015). The „CCC complex“ formed from these proteins has only been found in mammalian cell lines but my results from *D. discoideum* are a strong evidence that the CCC complex is an extraordinarily evolutionarily conserved component of the vesicular WASH complex machinery, probably common to all WASH complex-bearing eukaryotes.

As COMMD proteins modulate protein ubiquitination (Maine et al., 2007) and ubiquitination was shown to activate the WASH complex (Hao et al., 2013), it is extremely interesting to note that I discovered many other components of the ubiquitin machinery. This includes CSN5 and CSN7 components of the COP9 signalosome, cullin-3 as well as a TRIM3-like and a TRAF6-like ubiquitin ligase. Interestingly, mammalian TRIM3 was shown to be a part of an early endosomal CART (cytoskeleton-associated recycling or transport) complex, together with myosin V and actinin (Yan et al., 2005). The results show that the ubiquitination machinery is strongly associated with FAM21. It probably plays a role in regulation of protein sorting (Acconcia et al., 2009) rather than the prototypical “polyubiquitination” signal for degradation.

Several actin-associated proteins enriched in the FAM21 sample demonstrate the physical proximity of FAM21 to the actin cytoskeleton network at the vesicular surface. As these are enriched in FAM21 compared to MROH1 sample, I hypothesize that FAM21 indeed localizes to those actin-rich domains on endosomes that WASH complex is responsible for. It is very probable that these are indirect interaction partners of FAM21 binding via actin, although a direct interaction with some of the actin-associated proteins is theoretically feasible.

Some of the discovered interaction partners cannot be assigned a function. This includes discoidins, cytoskeleton-interacting and adhesion proteins known primarily from *D. discoideum* (Alexander et al., 1992; Springer et al., 1984) - but human counterparts, which transmit signals

from the extracellular matrix into the cell interior, have also recently sparked interest (Valiathan et al., 2012). No reports of discoidin localization to endosomes have been uncovered and this finding merits further research. A second example is FAM45, a well conserved protein (32% amino acid identity between *D. discoideum* and human) with no clue to its function available. Another group of enriched proteins represents nucleolar or nucleoli-associated proteins. I attribute this either to recent reports of FAM21 in the nucleus (Deng et al., 2014) or to mere artefacts caused by accidental autophagic destruction of the nucleoli during *D. discoideum* washing steps.

Crosslinking experiments are data-rich but can only provide us with a general list of interaction partners. To dissect the interactions happening specifically at LFa motifs I delineated a sequence in the C-terminal domain of *D. discoideum* FAM21 which included 7 LFa motifs. Pull-down from *D. discoideum* lysate uncovered some interaction partners of FAM21 that have already been published: CCDC22 and CCDC93 (Freeman et al., 2014; Phillips-Krawczak et al., 2015) and adaptor protein 2 complex (AP-2) α2 subunit (Jia et al., 2012). Other candidates are completely new to the field and include serine/threonine protein phosphatase PP1 and protein FAM45.

To determine if these interactions are evolutionarily conserved, I used the same approach and the same *D. discoideum* fragment to pull down interaction proteins from a U2OS cell lysate. The result was comparatively richer and suggests that the protein network at LFa motifs is well developed in mammalian cells. The qualitative difference between mass spectrometers used for the experiments can also be accounted for the higher number of detected proteins. Despite the fact that a *D. discoideum* sequence was used, I was able to confirm that the approx. 250 amino acid fragment is able to interact with a wide variety of established as well as new interaction proteins in the mammalian lysate. Most importantly, Vps35 was detected as an interaction partner of LFa motifs from *D. discoideum*. Detecting this protein from the U2OS lysate using *D. discoideum* fragment, while at the same time failing to detect it from *D. discoideum* lysate, strongly suggests that the notoriously known FAM21-Vps35 interaction (Harbour et al., 2012; Jia et al., 2012) is missing in *D. discoideum* cells. More sensitive search also uncovered retromer component VPS26B in the pulldown from the mammalian lysate. SNX27, a non-conventional sorting nexin, is a robust hit. I hypothesize that SNX27 is recruited to FAM21 LFa motifs and forms a functional module with retromer. Some studies have shown that SNX27 binds WASH complex which recruits it to the retromer (Temkin et al., 2011) while other authors

have demonstrated that SNX27 interacts with both WASH complex and the retromer (Steinberg et al., 2013).

Other detected interaction partners found in the mammalian lysate pull-down are new to the field. First and foremost, catalytic subunits α, β and γ of serine/threonine protein phosphatase PP1 were found. PP1 subunit alpha is the only protein found in crosslinking experiment as well as in the pull-down from both *D. discoideum* and U2OS cells. There is no publication suggesting that it interacts with the WASH complex. In cells, PP1 is bound by more than 200 regulatory proteins with a consensus binding sequence (K/R)(K/R)(V/I)X(F/W), 70 % of which are intrinsically disordered proteins - without clear secondary structure (Choy et al., 2012). FAM21 C-terminal domain is indeed intrinsically disordered and *D. discoideum* FAM21 includes a sequence RKVTF (amino acids 441-445) which complies with the consensus sequence. I therefore propose that *D. discoideum* FAM21 is a novel PP1-regulatory protein. The binding sequence is very well conserved among all sequenced *Dictyostelium* species but almost undetectable among more distantly related eukaryotes. Human FAM21C includes a somewhat similar sequence RKVQS (amino acids 474-478) which will be subjected to scrutiny in our future research in order to determine whether the FAM21-PP1 interaction is only specific to *Dictyostelium* FAM21 or represents a more general phenomenon.

Yet other hits of the pulldown from the mammalian lysate include liprin-β1 [liprins are poorly characterized proteins which were recently found to regulate actin branching activity of formins, (Sakamoto et al., 2012)] and myosin-IV heavy chain MYH4 [non-conventional myosin heavy chain IIB expressed in murine skeletal muscles but not in human muscle tissue (Kurapati et al., 2011), suggesting it could play a different role in the human body]. Rab proteins are usually very informative regarding the localization of proteins in the vesicular system. Detection of Rab14, found in an intermediate compartment between the Rab5-positive early endosome and the Rab11-positive recycling endosome (Linford et al., 2012), makes it a strong Rab candidate for presence on WASH complex-decorated early endosomal tubules. Remarkably, Rab14 was also found in the crosslinking assay in *D. discoideum*, suggesting its localization is evolutionarily conserved. How Rab14 is recruited to the GST-tagged FAM21 fragment is not currently clear. On the other hand, human CCDC93 and CCDC22 were not detected. – their binding to FAM21 could be due to sequence motifs not present in the *D. discoideum* FAM21 fragment, or their binding in humans is mediated by the C-terminal end of FAM21 only, as indeed shown recently (Phillips-Krawczak et al., 2015).

The number of interaction partners detected using a *D. discoideum* fragment incubated in a mammalian lysate is especially interesting because the corresponding mammalian sequence is very diverged from it. In fact, the LFa motifs are the only portions of the sequence that are truly conserved between *D. discoideum* and mammals. The findings underline the importance of LFa motifs for the FAM21 interaction network.

5. 3. Endosomal attachment of FAM21

The experiments have also provided several indirect lines of evidence which dispute the importance of Vps35-FAM21 interaction for WASH complex association with endosomes. First, Vps35 is not among the ~1601 proteins detected in the FAM21 crosslinking screen in *D. discoideum*. Still, the *D. discoideum* WASH complex is well associated with endosomes. If retromer component Vps35 was an important FAM21-interacting protein crucial for this localization, high amounts of Vps35 would be expected to appear in the results of the crosslinking screen, which is not biased towards certain proteins and does not discriminate proteins with a high dissociation constant (weakly binding). In conclusion, Vps35 is probably not required for the endosomal localization of FAM21 in *D. discoideum*.

I then asked the question whether this can be extrapolated to human cell lines. In contrast to *D. discoideum*, FAM21 indeed binds Vps35 in the human lysate, as shown using a GST pulldown approach with a FAM21 fragment from *D. discoideum*. However, knock-down of Vps35 does not lead to any profound changes in endosomal localization of FAM21. Most of FAM21 puncta remain localized to endosomes - early endosomes, late endosomes or lysosomes. This result is in a conflict with the widely accepted paradigm (Zavodszky et al., 2014) but is supported by at least one recent publication (McGough et al., 2014a). I hypothesize that there are additional factors holding FAM21 to the endosomes.

Moreover, microscopic experiments in the supplementary section of this thesis suggest that FAM21 does not localize to the endosomal membrane *per se*. It does not colocalize with a membrane marker, nor with the endosome-decorating actin patches. Rather, super-resolution imaging shows FAM21 as forming puncta around the endosomal actin patches. There are several explanations to this. FAM21 is either recruited to endosome tubules emanating from the centre of endosomes and retracting during the fixation step, or does not bind the membrane directly at all and is instead recruited to the actin patches around the membrane. This surprising finding will be addressed in future research at our laboratory.

In conclusion, these results strongly suggest that there are additional mechanisms [besides the retromer] which recruit the WASH complex to endosomes. This study only concentrated on protein FAM21 but in fact any component of the WASH complex could play a role in the endosomal association. SWIP knock-out *D. discoideum* has WASH completely delocalized to the cytosol (Park et al., 2013). Alternatively, the binding of the WASH complex could indeed be mediated by WASH VCA domain, if it was shown to selectively bind endosomal actin patches. Additional membrane- or actin-binding domains in WASH complex currently represent the most likely explanation for WASH complex endosomal recruitment.

Currently, mammalian cell studies usually point towards FAM21 C-terminal tail as the key mechanism behind WASH complex endosomal recruitment (Harbour et al., 2012; Helfer et al., 2013). Early publications have indicated that FAM21 binds phosphoinositides (Jia et al., 2010) but this model of FAM21 membrane recruitment is not often taken into consideration and the topic merits further study. The association of FAM21 with membrane or with actin patches on the membrane could also be due to other binding partners and indeed, some candidates were pinpointed even in this thesis. For example, the recently described CCC complex is here for the first time shown to be an evolutionary conserved binding partner of the WASH complex – however, recent data suggest that CCC complex association is strongly dependent on the WASH complex rather than vice versa (Phillips-Krawczak et al., 2015). At least in mammalian cells, sorting nexin 27 is an important binding partner of FAM21 and PX domain of SNX27 can associate with membrane by binding phosphatidylinositol-3-phosphate (Cai et al., 2011). Crosslinking experiment also demonstrated enrichment of a large number of prototypical actin-associated proteins which may form low-affinity binding sites for the WASH complex. Conceivably, the WASH complex forms a large pool (observed as FAM21 puncta) via low-affinity binding to actin or actin-binding proteins. A small portion of WASH complexes is then recruited to the endosomal membrane.

Remarkably, absence of retromer among the FAM21-interacting proteins in *D. discoideum* suggests that LFa motifs, present in the FAM21 sequence of both *D. discoideum* and humans, serve a more diverse role in cells than just binding the retromer. In this respect, it is interesting to note that metazoan FKBP15 also possesses an LFa motif at the C-terminus (own unpublished findings). Still, presence of ~20 unique sequence patterns in a single protein remains the biggest conundrum in FAM21 research.

6. Conclusion

New cellular roles have recently been assigned to the WASH complex, an endosomal pentameric complex which regulates vesicular traffic. I have demonstrated that FAM21, a pivotal WASH complex component, localizes to early, late and recycling endosomes as well as lysosomes. This widespread occurrence of FAM21 throughout the vesicular system has led me to inspect the interaction partners of the WASH complex because the currently recognized proteins cannot explain such diverse localization.

A search for new FAM21 interaction partners used several approaches either in *D. discoideum* or in mammalian cells and produced a rich dataset of candidates for further validation. Serine/threonine protein phosphatase 1 (PP1) was found to bind to *D. discoideum* FAM21 and this finding was explained by the discovery of a strong PP1-interaction motif in the sequence of *D. discoideum* FAM21. FAM21 thus may act as one of the >100 currently known intrinsically disordered PP1-regulatory proteins. Additionally, several already established partners were confirmed using these approaches. The CCC complex recently described in human cells has been shown to be present in *D. discoideum* for the first time. SNX27 and Rab14 were associated with a FAM21 C-terminal fragment consisting of several LFa motifs; this suggests that the LFa motifs are recruited to membrane tubules and associate with specific sorting nexins and Rab proteins.

In contrast, a retromer component Vps35 was not detected in a sensitive crosslinking screen in *D. discoideum*, questioning not only the published interaction with FAM21 but also the importance of retromer for the localization of WASH complex in eukaryotic cells. Results suggest that Vps35 interacts with FAM21 in human cells but not in *D. discoideum*. Vps35 was also found to be dispensable for WASH complex interaction with endosomes in human cells. Only a mild, statistically insignificant reduction of FAM21 localization to endosomes was found upon knock-down of Vps35.

Since the discovery of WASH in 2007, our understanding of the role of the WASH complex remains poor despite recent progress. Localization and interaction studies such as this show potential to provide new information of its physiological function. Understanding the WASH complex role will in future hopefully enable us to extrapolate it to serious medical conditions associated with the dysfunction of WASH complex components.

7. Acknowledgements

My dearest thanks go to Lenka Libusová who has introduced me to science and led my research for both my Bachelor's and Master's thesis. The list of other mentors and collaborators is long but I would like to thank all members of the Laboratory of Molecular Genetics of Development at Faculty of Science, Charles University in Prague as well as all members of Laboratory of Cell Migration and Chemotaxis at Beatson Institute, Glasgow, UK.

I am grateful to Robert Insall and Peter Thomason for enabling me to work at the Beatson Institute for Cancer Research and for their help with the whole *Dictyostelium* part of my project. My thanks also go to Matthew Seaman (University of Cambridge, UK) for GFP-tagged WASH complex constructs, Vojtěch Žíla (Laboratory of Virology, Faculty of Science, Charles University) for the Rab11-GFP construct, Edward De Robertis for the RFP-tagged Hrs construct and Tomáš Brabec for the FAM21-myc-his construct. I am very grateful to Jose Batista for his help with the crosslinking assay, Jan Ohotski for his help with the GST pulldown, Sergio Lilla and Karel Harant for mass spectrometry analysis, Ondřej Šebesta for help with fluorescence microscopy and image analysis, Ondřej Horváth and Ivan Novotný for help with SIM microscopy and Kristina Koudelová for the assistance with GST pulldown in mammalian cells.

8. Abbreviations

ADP adenosine diphosphate
AP-2 α2 adaptor protein 2 complex subunit α2
Arp2/3 actin-related proteins 2 and 3 complex
ATG9A autophagy-related protein 9A
ATP adenosine triphosphate
ATP7A ATPase 7A
BAR Bin-Amphiphysin-Rvs
BLOC-1 biogenesis of lysosome-related organelles complex 1
BSA bovine serum albumin
cAMP cyclic adenosine monophosphate
CapZα / β capping protein Z band α / β
CARMIL capping protein, Arp2/3 and myosin I linker
CART cytoskeleton-associated recycling or transport
CCC CCDC22-CCDC93-COMMD complex
CCDC22 / 53 / 93 coiled-coil domain containing protein 22 / 53 / 93
Cdc42 cell division control protein 42 homolog
CI-MPR cation-independent mannose phosphate receptor
CmfB conditioned medium factor receptor 1
COMMD copper metabolism MURR1 domain-containing protein 1

COP9 constitutive photomorphogenesis 9
CP capping protein
CSN5 / 7 COP9 subunit 5 / 7
DAPI 4',6-diamidino-2-phenylindole
DD7-1 discoidin domain 7-1
DMEM Dulbecco's modified Eagle medium
DNAJ *(referring or related to)* DnaJ protein or domain
EDTA ethylenediaminetetraacetic acid
EEA1 early endosomal antigen 1
Emg1 essential for mitotic growth 1
ER endoplasmic reticulum
ESCRT endosomal sorting complex required for transport
FAM21 / 45 family with sequence homology 21 / 45 protein
FKBP4 / 15 FK506 binding protein 4 / 15
GAPDH glyceraldehyde 3-phosphate dehydrogenase
GFP green fluorescent protein
GLUT1 glucose transporter 1
GNL2 guanine nucleotide binding protein-like 2
GST glutathione-S-transferase
GTPase guanosine triphosphatase
HEPES 4-(2-hydroxyethyl)-1-piperazine ethanesulfonic acid
HRP horseradish peroxidase
I-κB NF-κB inhibitor
JMY junction-mediating and regulatory protein
LAMP1 lysosomal-associated membrane protein 1
LB lysogeny broth
LC-MS/MS liquid chromatography – mass spectrometry
LFa leucine-phenylalanine-acidic
MAGE melanoma antigen
MHCII major histocompatibility complex II
MROH1 maestro heat-like repeat family member 1
MS mass spectrometry
MSB microtubule stabilizing buffer
MT1-MMP membrane type 1 matrix metalloproteinase
Murr1 murine U2af1-rs1 region
MYH4 myosin IIb heavy chain 4
NES nuclear export sequence
NF-κB nuclear factor kappa-light-chain-enhancer of activated B cells
NPF nucleation-promoting factor
PBS phosphate buffer saline
PCR polymerase chain reaction
PI(3)P phosphatidylinositol-3-phosphate
PIP phosphatidylinositol phosphate
PP1 serine/threonine protein phosphatase 1
PX phox
RBM28 RNA-binding protein 28
RFP red fluorescent protein
RFP44 RING finger protein 44
Rho ras homology
RING really interesting new gene

RME-8 receptor-mediated endocytosis-8
RPF2 ribosome production factor 2 homolog
SDS PAGE SDS polyacrylamide gel electrophoresis
SDS sodium dodecyl sulphate
SIM structured illumination microscopy
SNX sorting nexin
SOB super optimal broth
SWIP strumpellin and WASH interacting protein
TAE Tris-acetate EDTA
TAEB triethylammonium bicarbonate buffer
TRAF6 tumor necrosis factor receptor associated factor 6
TRIM3 / 27 tripartite motif 3 / 27
V-ATPase vacuolar adenosine triphosphatase
VCA verprolin-connector-acidic
Vps26 / 29 / 35 vacuolar protein sorting-associated protein 26 / 29 / 35
WAFL WASP and FKBP-like
WASH Wiscott-Aldrich syndrome homology
WASP Wiscott-Aldrich syndrome protein
WAVE / SCAR WASP family Verprolin-homologous protein/Suppressor of cAMP receptor
WHAMM WASP homolog-associated protein with actin, membranes and microtubules
WHD1 / WHD2 WASH homology domain 1 / 2

9. References

Acconcia, F., Sigismund, S., and Polo, S. (2009). Ubiquitin in trafficking: the network at work. Exp. Cell Res. *315*, 1610–1618.

Alexander, S., Sydow, L.M., Wessels, D., and Soll, D.R. (1992). Discoidin proteins of Dictyostelium are necessary for normal cytoskeletal organization and cellular morphology during aggregation. Differ. Res. Biol. Divers. *51*, 149–161.

Astbury, W.T., Perry, S.V., Reed, R., and Spark, L.C. (1947). An electron microscope and X-ray study of actin: I. Electron microscope. Biochim. Biophys. Acta *1*, 379–392.

Bache, K.G., Brech, A., Mehlum, A., and Stenmark, H. (2003). Hrs regulates multivesicular body formation via ESCRT recruitment to endosomes. J. Cell Biol. *162*, 435–442.

Baum, B., and Kunda, P. (2005). Actin nucleation: spire - actin nucleator in a class of its own. Curr. Biol. CB *15*, R305–R308.

Bear, J.E., Rawls, J.F., and Saxe, C.L. (1998). SCAR, a WASP-related Protein, Isolated as a Suppressor of Receptor Defects in Late Dictyostelium Development. J. Cell Biol. *142*, 1325–1335.

Blanchoin, L., and Pollard, T.D. (2002). Hydrolysis of ATP by polymerized actin depends on the bound divalent cation but not profilin. Biochemistry (Mosc.) *41*, 597–602.

Burd, C., and Cullen, P.J. (2014). Retromer: a master conductor of endosome sorting. Cold Spring Harb. Perspect. Biol. *6*.

Burke, T.A., Christensen, J.R., Barone, E., Suarez, C., Sirotkin, V., and Kovar, D.R. (2014). Homeostatic actin cytoskeleton networks are regulated by assembly factor competition for monomers. Curr. Biol. CB *24*, 579–585.

Cai, L., Loo, L.S., Atlashkin, V., Hanson, B.J., and Hong, W. (2011). Deficiency of Sorting Nexin 27 (SNX27) Leads to Growth Retardation and Elevated Levels of N-Methyl-d-Aspartate Receptor 2C (NR2C). Mol. Cell. Biol. *31*, 1734–1747.

Campellone, K.G., and Welch, M.D. (2010). A Nucleator Arms Race: Cellular Control of Actin Assembly. Nat. Rev. Mol. Cell Biol. *11*, 237–251.

Carnell, M., Zech, T., Calaminus, S.D., Ura, S., Hagedorn, M., Johnston, S.A., May, R.C., Soldati, T., Machesky, L.M., and Insall, R.H. (2011). Actin polymerization driven by WASH causes V-ATPase retrieval and vesicle neutralization before exocytosis. J. Cell Biol. *193*, 831–839.

Castano, E., Philimonenko, V.V., Kahle, M., Fukalová, J., Kalendová, A., Yildirim, S., Dzijak, R., Dingová-Krásna, H., and Hozák, P. (2010). Actin complexes in the cell nucleus: new stones in an old field. Histochem. Cell Biol. *133*, 607–626.

Chhabra, E.S., and Higgs, H.N. (2007). The many faces of actin: matching assembly factors with cellular structures. Nat. Cell Biol. *9*, 1110–1121.

Choudhury, A., Dominguez, M., Puri, V., Sharma, D.K., Narita, K., Wheatley, C.L., Marks, D.L., and Pagano, R.E. (2002). Rab proteins mediate Golgi transport of caveola-internalized glycosphingolipids and correct lipid trafficking in Niemann-Pick C cells. J. Clin. Invest. *109*, 1541–1550.

Choy, M.S., Page, R., and Peti, W. (2012). Regulation of protein phosphatase 1 by intrinsically disordered proteins. Biochem. Soc. Trans. *40*, 969–974.

Cullen, P.J., and Korswagen, H.C. (2012). Sorting nexins provide diversity for retromer-dependent trafficking events. Nat. Cell Biol. *14*, 29–37.

Dayel, M.J., Holleran, E.A., and Mullins, R.D. (2001). Arp2/3 complex requires hydrolyzable ATP for nucleation of new actin filaments. Proc. Natl. Acad. Sci. U. S. A. *98*, 14871–14876.

Deng, Z.-H., Gomez, T.S., Osborne, D.G., Phillips-Krawczak, C.A., Zhang, J.-S., and Billadeau, D.D. (2014). Nuclear localized FAM21 participates in NF-κB-dependent gene regulation in pancreatic cancer cells. J. Cell Sci. *128*, 373–384

Derivery, E., and Gautreau, A. (2010a). Evolutionary conservation of the WASH complex, an actin polymerization machine involved in endosomal fission. Commun. Integr. Biol. *3*, 227–230.

Derivery, E., and Gautreau, A. (2010b). Assaying WAVE and WASH complex constitutive activities toward the Arp2/3 complex. Methods Enzymol. *484*, 677–695.

Derivery, E., Sousa, C., Gautier, J.J., Lombard, B., Loew, D., and Gautreau, A. (2009). The Arp2/3 Activator WASH Controls the Fission of Endosomes through a Large Multiprotein Complex. Dev. Cell *17*, 712–723.

Derry, J.M., Ochs, H.D., and Francke, U. (1994). Isolation of a novel gene mutated in Wiskott-Aldrich syndrome. Cell *78*, 635–644.

Dingová, H., Fukalová, J., Maninová, M., Philimonenko, V.V., and Hozák, P. (2009). Ultrastructural localization of actin and actin-binding proteins in the nucleus. Histochem. Cell Biol. *131*, 425–434.

Eden, S., Rohatgi, R., Podtelejnikov, A.V., Mann, M., and Kirschner, M.W. (2002). Mechanism of regulation of WAVE1-induced actin nucleation by Rac1 and Nck. Nature *418*, 790–793.

Edwards, M., Zwolak, A., Schafer, D.A., Sept, D., Dominguez, R., and Cooper, J.A. (2014). Capping protein regulators fine-tune actin assembly dynamics. Nat. Rev. Mol. Cell Biol. *15*, 677–689.

Firat-Karalar, E.N., and Welch, M.D. (2011). New mechanisms and functions of actin nucleation. Curr. Opin. Cell Biol. *23*, 4–13.

Freeman, C., Seaman, M.N.J., and Reid, E. (2013). The hereditary spastic paraplegia protein strumpellin: characterisation in neurons and of the effect of disease mutations on WASH complex assembly and function. Biochim. Biophys. Acta *1832*, 160–173.

Freeman, C.L., Hesketh, G., and Seaman, M.N.J. (2014). RME-8 coordinates the activity of the WASH complex with the function of the retromer SNX dimer to control endosomal tubulation. J. Cell Sci. *127*, 2053–2070.

Galovic, M., Xu, D., Areces, L.B., van der Kammen, R., and Innocenti, M. (2011). Interplay between N-WASP and CK2 optimizes clathrin-mediated endocytosis of EGFR. J. Cell Sci. *124*, 2001–2012.

Gligorijevic, B., Wyckoff, J., Yamaguchi, H., Wang, Y., Roussos, E.T., and Condeelis, J. (2012). N-WASP-mediated invadopodium formation is involved in intravasation and lung metastasis of mammary tumors. J. Cell Sci. *125*, 724–734.

Goley, E.D., and Welch, M.D. (2006). The ARP2/3 complex: an actin nucleator comes of age. Nat. Rev. Mol. Cell Biol. *7*, 713–726.

Gomez, T.S., and Billadeau, D.D. (2009). A FAM21-containing WASH complex regulates retromer-dependent sorting. Dev. Cell *17*, 699–711.

Gomez, T.S., Gorman, J.A., de Narvajas, A.A.-M., Koenig, A.O., and Billadeau, D.D. (2012). Trafficking defects in WASH-knockout fibroblasts originate from collapsed endosomal and lysosomal networks. Mol. Biol. Cell *23*, 3215–3228.

Graham, D.B., Osborne, D.G., Piotrowski, J.T., Gomez, T.S., Gmyrek, G.B., Akilesh, H.M., Dani, A., Billadeau, D.D., and Swat, W. (2014). Dendritic Cells Utilize the Evolutionarily Conserved WASH and Retromer Complexes to Promote MHCII Recycling and Helper T Cell Priming. PloS One *9*, e98606.

Hänisch, J., Ehinger, J., Ladwein, M., Rohde, M., Derivery, E., Bosse, T., Steffen, A., Bumann, D., Misselwitz, B., Hardt, W.-D., et al. (2010). Molecular dissection of Salmonella-induced membrane ruffling versus invasion. Cell. Microbiol. *12*, 84–98.

Hao, Y.-H., Doyle, J.M., Ramanathan, S., Gomez, T.S., Jia, D., Xu, M., Chen, Z.J., Billadeau, D.D., Rosen, M.K., and Potts, P.R. (2013). Regulation of WASH-Dependent Actin Polymerization and Protein Trafficking by Ubiquitination. Cell *152*, 1051–1064.

Harbour, M.E., Breusegem, S.Y.A., Antrobus, R., Freeman, C., Reid, E., and Seaman, M.N.J. (2010). The cargo-selective retromer complex is a recruiting hub for protein complexes that regulate endosomal tubule dynamics. J. Cell Sci. *123*, 3703–3717.

Harbour, M.E., Breusegem, S.Y., and Seaman, M.N.J. (2012). Recruitment of the endosomal WASH complex is mediated by the extended “tail” of Fam21 binding to the retromer protein Vps35. Biochem. J. *442*, 209–220.

Harrison, M.S., Hung, C.-S., Liu, T., Christiano, R., Walther, T.C., and Burd, C.G. (2014). A mechanism for retromer endosomal coat complex assembly with cargo. Proc. Natl. Acad. Sci. U. S. A. *111*, 267–272.

Harterink, M., Port, F., Lorenowicz, M.J., McGough, I.J., Silhankova, M., Betist, M.C., van Weering, J.R.T., van Heesbeen, R.G.H.P., Middelkoop, T.C., Basler, K., et al. (2011). A SNX3-dependent retromer pathway mediates retrograde transport of the Wnt sorting receptor Wntless and is required for Wnt secretion. Nat. Cell Biol. *13*, 914–923.

Helfer, E., Harbour, M.E., Henriot, V., Lakisic, G., Sousa-Blin, C., Volceanov, L., Seaman, M.N.J., and Gautreau, A. (2013). Endosomal recruitment of the WASH complex: active sequences and mutations impairing interaction with the retromer. Biol. Cell Auspices Eur. Cell Biol. Organ. *105*, 191–207.

Huang, C.-Y., Lu, T.-Y., Bair, C.-H., Chang, Y.-S., Jwo, J.-K., and Chang, W. (2008). A Novel Cellular Protein, VPEF, Facilitates Vaccinia Virus Penetration into HeLa Cells through Fluid Phase Endocytosis. J. Virol. *82*, 7988–7999.

Insall, R.H. (2013). WASH complex conservation: don't WASH away the family! Trends Cell Biol. *23*, 519–520.

Ismail, A.M., Padrick, S.B., Chen, B., Umetani, J., and Rosen, M.K. (2009). The WAVE regulatory complex is inhibited. Nat. Struct. Mol. Biol. *16*, 561–563.

Jia, D., Gomez, T.S., Metlagel, Z., Umetani, J., Otwinowski, Z., Rosen, M.K., and Billadeau, D.D. (2010). WASH and WAVE actin regulators of the Wiskott–Aldrich syndrome protein (WASP) family are controlled by analogous structurally related complexes. Proc. Natl. Acad. Sci. *107*, 10442–10447.

Jia, D., Gomez, T.S., Billadeau, D.D., and Rosen, M.K. (2012). Multiple repeat elements within the FAM21 tail link the WASH actin regulatory complex to the retromer. Mol. Biol. Cell *23*, 2352–2361.

Jovic, M., Sharma, M., Rahajeng, J., and Caplan, S. (2010). The early endosome: a busy sorting station for proteins at the crossroads. Histol. Histopathol. *25*, 99–112.

Kabsch, W., Mannherz, H.G., Suck, D., Pai, E.F., and Holmes, K.C. (1990). Atomic structure of the actin:DNase I complex. Nature *347*, 37–44.

Kelleher, J.F., Atkinson, S.J., and Pollard, T.D. (1995). Sequences, structural models, and cellular localization of the actin-related proteins Arp2 and Arp3 from Acanthamoeba. J. Cell Biol. *131*, 385–397.

King, J.S., Gueho, A., Hagedorn, M., Gopaldass, N., Leuba, F., Soldati, T., and Insall, R.H. (2013). WASH is required for lysosomal recycling and efficient autophagic and phagocytic digestion. Mol. Biol. Cell *24*, 2714–2726.

Komada, M., and Kitamura, N. (1995). Growth factor-induced tyrosine phosphorylation of Hrs, a novel 115-kilodalton protein with a structurally conserved putative zinc finger domain. Mol. Cell. Biol. *15*, 6213–6221.

Kovar, D.R. (2006). Molecular details of formin-mediated actin assembly. Curr. Opin. Cell Biol. *18*, 11–17.

Kumar, C., and Mann, M. (2009). Bioinformatics analysis of mass spectrometry-based proteomics data sets. FEBS Lett. *583*, 1703–1712.

Kunda, P., Craig, G., Dominguez, V., and Baum, B. (2003). Abi, Sra1, and Kette control the stability and localization of SCAR/WAVE to regulate the formation of actin-based protrusions. Curr. Biol. CB *13*, 1867–1875.

Kurapati, R., McKenna, C., Lindqvist, J., Williams, D., Simon, M., LeProust, E., Baker, J., Cheeseman, M., Carroll, N., Denny, P., et al. (2011). Myofibrillar myopathy caused by a mutation in the motor domain of mouse MyHC IIb. Hum. Mol. Genet. ddr605.

Li, S., Armstrong, C.M., Bertin, N., Ge, H., Milstein, S., Boxem, M., Vidalain, P.-O., Han, J.-D.J., Chesneau, A., Hao, T., et al. (2004). A map of the interactome network of the metazoan C. elegans. Science *303*, 540–543.

Linardopoulou, E.V., Parghi, S.S., Friedman, C., Osborn, G.E., Parkhurst, S.M., and Trask, B.J. (2007). Human subtelomeric WASH genes encode a new subclass of the WASP family. PLoS Genet. *3*, e237.

Linford, A., Yoshimura, S., Bastos, R.N., Langemeyer, L., Gerondopoulos, A., Rigden, D.J., and Barr, F.A. (2012). Rab14 and Its Exchange Factor FAM116 Link Endocytic Recycling and Adherens Junction Stability in Migrating Cells. Dev. Cell *22-540*, 952–966.

Lorenz, M., Yamaguchi, H., Wang, Y., Singer, R.H., and Condeelis, J. (2004). Imaging sites of N-wasp activity in lamellipodia and invadopodia of carcinoma cells. Curr. Biol. CB *14*, 697–703.

Lukas, J.R., Aigner, M., Denk, M., Heinzl, H., Burian, M., and Mayr, R. (1998). Carbocyanine postmortem neuronal tracing. Influence of different parameters on tracing distance and combination with immunocytochemistry. J. Histochem. Cytochem. Off. J. Histochem. Soc. *46*, 901–910.

Machesky, L.M., Atkinson, S.J., Ampe, C., Vandekerckhove, J., and Pollard, T.D. (1994). Purification of a cortical complex containing two unconventional actins from Acanthamoeba by affinity chromatography on profilin-agarose. J. Cell Biol. *127*, 107–115.

Maine, G.N., Mao, X., Komarck, C.M., and Burstein, E. (2007). COMMD1 promotes the ubiquitination of NF-kappaB subunits through a cullin-containing ubiquitin ligase. EMBO J. *26*, 436–447.

Maniak, M. (2011). Dictyostelium as a model for human lysosomal and trafficking diseases. Semin. Cell Dev. Biol. *22*, 114–119.

Mao, X., Gluck, N., Chen, B., Starokadomskyy, P., Li, H., Maine, G.N., and Burstein, E. (2011). COMMD1 (copper metabolism MURR1 domain-containing protein 1) regulates Cullin RING ligases by preventing CAND1 (Cullin-associated Nedd8-dissociated protein 1) binding. J. Biol. Chem. *286*, 32355–32365.

McGough, I.J., Steinberg, F., Jia, D., Barbuti, P.A., McMillan, K.J., Heesom, K.J., Whone, A.L., Caldwell, M.A., Billadeau, D.D., Rosen, M.K., et al. (2014a). Retromer Binding to FAM21 and the WASH Complex Is Perturbed by the Parkinson Disease-Linked VPS35(D620N) Mutation. Curr. Biol. *24*, 1670–1676.

McGough, I.J., Steinberg, F., Gallon, M., Yatsu, A., Ohbayashi, N., Heesom, K.J., Fukuda, M., and Cullen, P.J. (2014b). Identification of molecular heterogeneity in SNX27-retromer-mediated endosome-to-plasma-membrane recycling. J. Cell Sci. *127*, 4940–4953.

Miki, H., Suetsugu, S., and Takenawa, T. (1998). WAVE, a novel WASP-family protein involved in actin reorganization induced by Rac. EMBO J. *17*, 6932–6941.

Monteiro, P., Rossé, C., Castro-Castro, A., Irondelle, M., Lagoutte, E., Paul-Gilloteaux, P., Desnos, C., Formstecher, E., Darchen, F., Perrais, D., et al. (2013). Endosomal WASH and exocyst complexes control exocytosis of MT1-MMP at invadopodia. J. Cell Biol. *203*, 1063–1079.

Mu, F.T., Callaghan, J.M., Steele-Mortimer, O., Stenmark, H., Parton, R.G., Campbell, P.L., McCluskey, J., Yeo, J.P., Tock, E.P., and Toh, B.H. (1995). EEA1, an early endosome-associated protein. EEA1 is a conserved alpha-helical peripheral membrane protein flanked by cysteine "fingers" and contains a calmodulin-binding IQ motif. J. Biol. Chem. *270*, 13503–13511.

Mullins, R.D., Heuser, J.A., and Pollard, T.D. (1998). The interaction of Arp2/3 complex with actin: nucleation, high affinity pointed end capping, and formation of branching networks of filaments. Proc. Natl. Acad. Sci. U. S. A. *95*, 6181–6186.

Neuhaus, E.M., Almers, W., and Soldati, T. (2002). Morphology and Dynamics of the Endocytic Pathway in Dictyostelium discoideum. Mol. Biol. Cell *13*, 1390–1407.

Nonoyama, S., and Ochs, H.D. (1998). Characterization of the Wiskott-Aldrich syndrome protein and its role in the disease. Curr. Opin. Immunol. *10*, 407–412.

Nozumi, M., Nakagawa, H., Miki, H., Takenawa, T., and Miyamoto, S. (2003). Differential localization of WAVE isoforms in filopodia and lamellipodia of the neuronal growth cone. J. Cell Sci. *116*, 239–246.

Oser, M., Yamaguchi, H., Mader, C.C., Bravo-Cordero, J.J., Arias, M., Chen, X., Desmarais, V., van Rheenen, J., Koleske, A.J., and Condeelis, J. (2009). Cortactin regulates cofilin and N-WASp activities to control the stages of invadopodium assembly and maturation. J. Cell Biol. *186*, 571–587.

Park, L., Thomason, P.A., Zech, T., King, J.S., Veltman, D.M., Carnell, M., Ura, S., Machesky, L.M., and Insall, R.H. (2013). Cyclical action of the WASH complex: FAM21 and capping protein drive WASH recycling, not initial recruitment. Dev. Cell *24*, 169–181.

Petryszak, R., Burdett, T., Fiorelli, B., Fonseca, N.A., Gonzalez-Porta, M., Hastings, E., Huber, W., Jupp, S., Keays, M., Kryvych, N., et al. (2014). Expression Atlas update--a database of gene and transcript expression from microarray- and sequencing-based functional genomics experiments. Nucleic Acids Res. *42*, D926–D932.

Phillips-Krawczak, C.A., Singla, A., Starokadomskyy, P., Deng, Z., Osborne, D.G., Li, H., Dick, C.J., Gomez, T.S., Koenecke, M., Zhang, J.-S., et al. (2015). COMMD1 is linked to the WASH complex and regulates endosomal trafficking of the copper transporter ATP7A. Mol. Biol. Cell *26*, 91–103.

Pollitt, A.Y., and Insall, R.H. (2009). WASP and SCAR/WAVE proteins: the drivers of actin assembly. J. Cell Sci. *122*, 2575–2578.

Qurashi, A., Sahin, H.B., Carrera, P., Gautreau, A., Schenck, A., and Giangrande, A. (2007). HSPC300 and its role in neuronal connectivity. Neural Develop. *2*, 18.

Reisler, E., and Egelman, E.H. (2007). Actin structure and function: what we still do not understand. J. Biol. Chem. *282*, 36133–36137.

Dos Remedios, C.G., Chhabra, D., Kekic, M., Dedova, I.V., Tsubakihara, M., Berry, D.A., and Nosworthy, N.J. (2003). Actin binding proteins: regulation of cytoskeletal microfilaments. Physiol. Rev. *83*, 433–473.

De Renzis, S., Sönnichsen, B., and Zerial, M. (2002). Divalent Rab effectors regulate the sub-compartmental organization and sorting of early endosomes. Nat. Cell Biol. *4*, 124–133.

Rohatgi, R., Ma, L., Miki, H., Lopez, M., Kirchhausen, T., Takenawa, T., and Kirschner, M.W. (1999). The interaction between N-WASP and the Arp2/3 complex links Cdc42-dependent signals to actin assembly. Cell *97*, 221–231.

Rojas, R., Kametaka, S., Haft, C.R., and Bonifacino, J.S. (2007). Interchangeable but Essential Functions of SNX1 and SNX2 in the Association of Retromer with Endosomes and the Trafficking of Mannose 6-Phosphate Receptors. Mol. Cell. Biol. *27*, 1112–1124.

Ropers, F., Derivery, E., Hu, H., Garshasbi, M., Karbasiyan, M., Herold, M., Nürnberg, G., Ullmann, R., Gautreau, A., Sperling, K., et al. (2011). Identification of a novel candidate gene for non-syndromic autosomal recessive intellectual disability: the WASH complex member SWIP. Hum. Mol. Genet. *20*, 2585–2590.

Rottner, K., Hänisch, J., and Campellone, K.G. (2010). WASH, WHAMM and JMY: regulation of Arp2/3 complex and beyond. Trends Cell Biol. *20*, 650–661.

Rotty, J.D., Wu, C., and Bear, J.E. (2013). New insights into the regulation and cellular functions of the ARP2/3 complex. Nat. Rev. Mol. Cell Biol. *14*, 7–12.

Rowland, A.A., Chitwood, P.J., Phillips, M.J., and Voeltz, G.K. (2014). ER Contact Sites Define the Position and Timing of Endosome Fission. Cell *159*, 1027–1041.

Ryder, P.V., Vistein, R., Gokhale, A., Seaman, M.N., Puthenveedu, M.A., and Faundez, V. (2013). The WASH complex, an endosomal Arp2/3 activator, interacts with the Hermansky-Pudlak syndrome complex BLOC-1 and its cargo phosphatidylinositol-4-kinase type IIα. Mol. Biol. Cell *24*, 2269–2284.

Sakamoto, S., Narumiya, S., and Ishizaki, T. (2012). A new role of multi scaffold protein Liprin-α. Bioarchitecture *2*, 43–49.

Schou, K.B., Andersen, J.S., and Pedersen, L.B. (2014). A divergent calponin homology (NN-CH) domain defines a novel family: implications for evolution of ciliary IFT complex B proteins. Bioinforma. Oxf. Engl. *30*, 899–902.

Seaman, M.N.J., Gautreau, A., and Billadeau, D.D. (2013). Retromer-mediated endosomal protein sorting: all WASHed up! Trends Cell Biol. *23*, 522–528.

Sept, D., and McCammon, J.A. (2001). Thermodynamics and kinetics of actin filament nucleation. Biophys. J. *81*, 667–674.

Simonsen, A., Lippé, R., Christoforidis, S., Gaullier, J.M., Brech, A., Callaghan, J., Toh, B.H., Murphy, C., Zerial, M., and Stenmark, H. (1998). EEA1 links PI(3)K function to Rab5 regulation of endosome fusion. Nature *394*, 494–498.

Springer, W.R., Cooper, D.N., and Barondes, S.H. (1984). Discoidin I is implicated in cell-substratum attachment and ordered cell migration of Dictyostelium discoideum and resembles fibronectin. Cell *39*, 557–564.

Starokadomskyy, P., Gluck, N., Li, H., Chen, B., Wallis, M., Maine, G.N., Mao, X., Zaidi, I.W., Hein, M.Y., McDonald, F.J., et al. (2013). CCDC22 deficiency in humans blunts activation of proinflammatory NF-κB signaling. J. Clin. Invest. *123*, 2244–2256.

Steinberg, F., Gallon, M., Winfield, M., Thomas, E.C., Bell, A.J., Heesom, K.J., Tavaré, J.M., and Cullen, P.J. (2013). A global analysis of SNX27-retromer assembly and cargo specificity reveals a function in glucose and metal ion transport. Nat. Cell Biol. *15*, 461–471.

Stes, E., Laga, M., Walton, A., Samyn, N., Timmerman, E., De Smet, I., Goormachtig, S., and Gevaert, K. (2014). A COFRADIC protocol to study protein ubiquitination. J. Proteome Res. *13*, 3107–3113.

Straub, F.B. (1942). Actin. Stud Inst Med Chem Univ Szeged *2*, 3.

Straub, F.B., and Feuer, G. (1950). Adenosine triphosphate, the functional group of actin. Kísérletes Orvtud. *2*, 141–151.

Sukumvanich, P., DesMarais, V., Sarmiento, C.V., Wang, Y., Ichetovkin, I., Mouneimne, G., Almo, S., and Condeelis, J. (2004). Cellular localization of activated N-WASP using a conformation-sensitive antibody. Cell Motil. Cytoskeleton *59*, 141–152.

Szymanski, C.J., William H. Humphries, I.V., and Payne, C.K. (2011). Single particle tracking as a method to resolve differences in highly colocalized proteins. Analyst *136*, 3527–3533.

Taelman, V.F., Dobrowolski, R., Plouhinec, J.-L., Fuentealba, L.C., Vorwald, P.P., Gumper, I., Sabatini, D.D., and De Robertis, E.M. (2010). Wnt signaling requires sequestration of glycogen synthase kinase 3 inside multivesicular endosomes. Cell *143*, 1136–1148.

Temkin, P., Lauffer, B., Jäger, S., Cimermancic, P., Krogan, N.J., and von Zastrow, M. (2011). SNX27 mediates retromer tubule entry and endosome-to-plasma membrane trafficking of signalling receptors. Nat. Cell Biol. *13*, 715–721.

Thompson, J.W., Nagel, J., Hoving, S., Gerrits, B., Bauer, A., Thomas, J.R., Kirschner, M.W., Schirle, M., and Luchansky, S.J. (2014). Quantitative Lys-ϵ-Gly-Gly (diGly) proteomics coupled with inducible RNAi reveals ubiquitin-mediated proteolysis of DNA damage-inducible transcript 4 (DDIT4) by the E3 ligase HUWE1. J. Biol. Chem. *289*, 28942–28955.

Tomasevic, N., Jia, Z., Russell, A., Fujii, T., Hartman, J.J., Clancy, S., Wang, M., Beraud, C., Wood, K.W., and Sakowicz, R. (2007). Differential Regulation of WASP and N-WASP by Cdc42, Rac1, Nck, and PI(4,5)P2. Biochemistry (Mosc.) *46*, 3494–3502.

Valdmanis, P.N., Meijer, I.A., Reynolds, A., Lei, A., MacLeod, P., Schlesinger, D., Zatz, M., Reid, E., Dion, P.A., Drapeau, P., et al. (2007). Mutations in the KIAA0196 gene at the SPG8 locus cause hereditary spastic paraplegia. Am. J. Hum. Genet. *80*, 152–161.

Valiathan, R.R., Marco, M., Leitinger, B., Kleer, C.G., and Fridman, R. (2012). Discoidin domain receptor tyrosine kinases: new players in cancer progression. Cancer Metastasis Rev. *31*, 295–321.

Veltman, D.M., and Insall, R.H. (2010). WASP family proteins: their evolution and its physiological implications. Mol. Biol. Cell *21*, 2880–2893.

Verboon, J.M., Rahe, T.K., Rodriguez-Mesa, E., and Parkhurst, S.M. (2015). Wash functions downstream of Rho1 GTPase in a subset of Drosophila immune cell developmental migrations. Mol. Biol. Cell. *26*, 1665–1674.

Weaver, A.M., Karginov, A.V., Kinley, A.W., Weed, S.A., Li, Y., Parsons, J.T., and Cooper, J.A. (2001). Cortactin promotes and stabilizes Arp2/3-induced actin filament network formation. Curr. Biol. CB *11*, 370–374.

Wegner, A. (1976). Head to tail polymerization of actin. J. Mol. Biol. *108*, 139–150.

Xhabija, B., Taylor, G.S., Fujibayashi, A., Sekiguchi, K., and Vacratsis, P.O. (2011). Receptor mediated endocytosis 8 is a novel PI(3)P binding protein regulated by myotubularin-related 2. FEBS Lett. *585*, 1722–1728.

Yan, Q., Sun, W., Kujala, P., Lotfi, Y., Vida, T.A., and Bean, A.J. (2005). CART: An Hrs/Actinin-4/BERP/Myosin V Protein Complex Required for Efficient Receptor Recycling. Mol. Biol. Cell *16*, 2470–2482.

Zavodszky, E., Seaman, M.N.J., Moreau, K., Jimenez-Sanchez, M., Breusegem, S.Y., Harbour, M.E., and Rubinsztein, D.C. (2014). Mutation in VPS35 associated with Parkinson's disease impairs WASH complex association and inhibits autophagy. Nat. Commun. *5*.

Zech, T., Calaminus, S.D.J., Caswell, P., Spence, H.J., Carnell, M., Insall, R.H., Norman, J., and Machesky, L.M. (2011). The Arp2/3 activator WASH regulates α5β1-integrin-mediated invasive migration. J. Cell Sci. *124*, 3753–3759.

Zuchero, J.B., Coutts, A.S., Quinlan, M.E., La Thangue, N.B., and Mullins, R.D. (2009). p53-cofactor JMY is a Multifunctional Actin Nucleation Factor. Nat. Cell Biol. *11*, 451–459.